

Manuscript version: Author's Accepted Manuscript

The version presented in WRAP is the author's accepted manuscript and may differ from the published version or Version of Record.

Persistent WRAP URL:

<http://wrap.warwick.ac.uk/154783>

How to cite:

Please refer to published version for the most recent bibliographic citation information. If a published version is known of, the repository item page linked to above, will contain details on accessing it.

Copyright and reuse:

The Warwick Research Archive Portal (WRAP) makes this work by researchers of the University of Warwick available open access under the following conditions.

© 2021 Elsevier. Licensed under the Creative Commons Attribution-NonCommercial-NoDerivatives 4.0 International <http://creativecommons.org/licenses/by-nc-nd/4.0/>.



Publisher's statement:

Please refer to the repository item page, publisher's statement section, for further information.

For more information, please contact the WRAP Team at: wrap@warwick.ac.uk.

Local stability of normal and high strength steel plates at elevated temperatures

Merih Kucukler

School of Engineering, University of Warwick, Coventry, CV4 7AL, UK

Abstract

This paper presents an investigation into the local buckling behaviour and design of normal and high strength steel plates at elevated temperatures. The considered high strength steel grades include grades S690 and S460 as well as the normal strength grades S355, S275 and S235 taken into consideration. Shell finite element models of normal and high strength steel plates are created to mimic their local buckling response in fire, whose accuracy is validated against experimental results from the literature. Extensive numerical parametric studies are then carried out by means of the validated finite element models, taking into account different plate slendernesses, elevated temperature levels, edge boundary conditions and steel grades. The accuracy of the design provisions provided in the current European structural steel fire design standard EN 1993-1-2 and its upcoming version prEN 1993-1-2 for the consideration of the local buckling behaviour of normal and high strength steel plates in fire is investigated. It is observed that the existing design rules given in both EN 1993-1-2 and prEN 1993-1-2 lead to rather scattered estimations of the local buckling strengths of high strength steel plates at elevated temperatures. New cross-section classification rules and effective width design equations for the ultimate strength predictions of normal and high strength steel plates in fire are developed. High accuracy and reliability of the proposed design rules are demonstrated.

Keywords: Cross-section classification, Effective width method, FE modelling, Fire, Geometric imperfections, High strength steel, Local buckling, S460, S690

1. Introduction

Categorised as steels whose yield strengths are larger than 460 MPa according to EN 1993-1-12 [1] and 450 MPa according to AS 4100 [2], high strength steels offer unique advantages to the construction industry such as reduced material consumptions and lighter self-weights for structural steel members, thereby enabling reduced carbon footprints for steel structures as well as lower transportation and construction costs. Enhanced yield strengths of high strength steels typically result in slender cross-sections for high strength

Email address: merih.kucukler@warwick.ac.uk (Merih Kucukler)

steel members, making them prone to local buckling effects which preclude the attainment of their full cross-section resistances. The local buckling behaviour of high strength steel members at room temperature has attracted significant research interest in recent years [3–10]. However, the previous research into the local buckling response of high strength steel elements at elevated temperatures, which is expected to be considerably different than their room temperature local buckling behaviour, is very limited [11–13].

To investigate the local buckling response of structural steel elements at elevated temperatures, a number of research studies have been performed in the literature. Yang et al. [14, 15], Hirashima and Uesugi [16], Dharma and Tan [17], Pauli et al. [18, 19], Wang et al. [20] and Prachar et al. [21] performed a series of experiments on the local buckling behaviour of steel members subjected to axial compression or bending in fire. In addition to these experimental investigations [14–21], numerical research studies into the local buckling response of steel elements in fire have also been carried out [11–13, 22–27], where the accuracy of the existing structural steel fire design standards [28, 29] was assessed. Amongst these studies [11–13, 22–27], Quiel and Garlock [22] and Couto et al. [25] put forward new effective width formulations for the determination of the effective section properties and local buckling strengths of steel members in fire. In the latter study [25], the limitations of the use of room temperature effective width equations for the determination of the local buckling strengths of steel sections in fire as recommended in EN 1993-1-2 [28] are highlighted. The effective width method put forward in Couto et al. [25] will appear in the upcoming version of EN 1993-1-2 [28] with modifications [26], which is currently referred to as prEN 1993-1-2 [30]. Even though there exist experimental and numerical research into the local buckling response of steel elements at elevated temperatures in the literature, in the aforementioned studies [12, 13, 22–27], neither the local buckling behaviour of high strength steel plates in fire was comprehensively investigated, nor has a new effective width method capable of furnishing accurate estimations of the ultimate resistances of high strength steel plates at elevated temperatures been established. It is also worth noting that in view of the somewhat limited research carried out on the topic, the local buckling behaviour of normal strength steel plates at elevated temperatures also warrants a careful examination, with the assessment of the existing design provisions given in structural steel design standards [28, 30].

For the purpose of exploring the local buckling behaviour of normal and high strength steel plates in fire, a comprehensive numerical research study is carried out in this paper. The high strength steel grades of S690 and S460 and the normal strength steel grades of S355, S275 and S235 are taken into consideration. Shell finite element models of steel plates able to replicate their response at elevated temperatures are created, whose accuracy is validated against experimental results from the literature. Carrying out the Geometrically and Materially Nonlinear Analyses with Imperfections (GMNIA) of the validated shell finite element models, extensive numerical parametric studies are then performed, taking into account different elevated temperature levels, plate slendernesses, edge boundary conditions and steel grades. A new cross-section classification approach and effective width method for the determination of the ultimate strengths of steel plates at elevated temperatures is proposed, whose accuracy and safety are verified against the results from nonlinear shell

finite element modelling. It is also shown that the proposed effective width method leads to improved accuracy relative to the effective width methods provided in EN 1993-1-2 [28] and prEN 1993-1-2 [30] for the predictions of the ultimate resistances of high strength steel plates in fire. Finally, the reliability analyses of the proposed design rules and the local buckling assessment provisions provided in EN 1993-1-2 [28] and prEN 1993-1-2 [30] are carried out, verifying the higher level of reliability of the proposed design approach relative to the provisions of EN 1993-1-2 [28] and prEN1993-1-2 [30] for the local buckling assessment of normal and high strength steel plates at elevated temperatures.

2. Finite element modelling

In this section, shell finite element models of normal and high strength steel plates able to replicate their local buckling response at elevated temperatures are created and validated against experimental results from the literature. Through the validated finite element models, extensive numerical parametric studies are then carried out, whose results will be used in the following sections for (i) the investigation of the accuracy of the existing design methods and (ii) the development of a new effective width design approach for the local buckling assessment of normal and high strength steel plates in fire.

2.1. Element type and modelling assumptions

Finite element models of steel plates were created by means of the finite element analysis software Abaqus [31] in this paper. In accordance with Xing et al. [32], two types of steel plates were taken into consideration: (i) a 1600 mm \times 400 mm plate whose both longitudinal edges are simply-supported, replicating the behaviour of the internal elements within steel cross-sections and (ii) a 4000 mm \times 400 mm plate whose one longitudinal edge is simply-supported and other longitudinal edge is free, which mimics the response of outstand flanges of open steel cross-sections. Note that while the dimensions of the internal plate elements used in this paper were in accordance with those adopted in Couto et al. [25], an aspect ratio of ten was utilised for outstand flange elements in line with [32] to achieve elastic critical buckling stresses that are closer to those determined through analytical solutions [33–35], considering that the elastic buckling stresses of outstand plate elements are sensitive to length effects and reduce with increasing aspect ratios. A four-node reduced integration shell element, which is designated as S4R in the Abaqus [31] element library and takes account of membrane strains and transverse shear deformations, was utilised in all finite element simulations. This element type has previously been adopted to mimic the behaviour of structural steel elements in similar applications [36–41]. In the shell finite element models, the element size of 20 mm \times 20 mm, corresponding to 20 elements along the 400 mm plate width, was used on the basis of a mesh sensitivity study. Unless otherwise indicated, in all the considered cases, isothermal analyses of the finite element models were carried out, assuming an initial uniform temperature increase to a predefined temperature value θ , which was represented by the modification of the material response, and then applying the loading at the designated elevated temperature level θ . For the purpose of tracing the full load-displacement response of the plates including the post-ultimate behaviour, the modified Riks analysis [42, 43] was utilised in all simulations.

2.2. Material modelling

With the aim of replicating the elevated temperature response of normal strength grade S355, S275 and S235 steel plates, the four-stage elevated temperature material model provided in EN 1993-1-2 [28] for carbon steel was employed, where the elevated temperature stress versus strain relationship was defined by means of the following equations:

$$\begin{aligned} \sigma &= \epsilon E_\theta \quad \text{for } \epsilon \leq \epsilon_{p,\theta}, \\ \sigma &= f_{p,\theta} - c + (b/a) \sqrt{a^2 - (\epsilon_{y,\theta} - \epsilon)^2} \quad \text{for } \epsilon_{p,\theta} \leq \epsilon \leq \epsilon_{y,\theta}, \\ \sigma &= f_{y,\theta} \quad \text{for } \epsilon_{y,\theta} \leq \epsilon \leq \epsilon_{t,\theta}, \\ \sigma &= f_{y,\theta} [1 - (\epsilon - \epsilon_{t,\theta}) / (\epsilon_{u,\theta} - \epsilon_{t,\theta})] \quad \text{for } \epsilon_{t,\theta} \leq \epsilon \leq \epsilon_{u,\theta}, \end{aligned} \quad (1)$$

in which σ and ϵ are the engineering stress and strain and E_θ , $f_{p,\theta}$ and $f_{y,\theta}$ are the Young's modulus, the proportional limit and the effective yield strength at temperature θ , respectively. In eq. (1), $\epsilon_{p,\theta}$ is the strain at proportional limit calculated as $\epsilon_{p,\theta} = f_{p,\theta}/E_\theta$, $\epsilon_{y,\theta}$ is the yield strain equal to 0.02 (i.e. $\epsilon_{y,\theta} = 0.02$), $\epsilon_{t,\theta}$ is the limiting strain for yield strength taken as 0.15 (i.e. $\epsilon_{t,\theta} = 0.15$) and $\epsilon_{u,\theta}$ is the ultimate strain equal to 0.20 (i.e. $\epsilon_{u,\theta} = 0.20$). The auxiliary coefficients a , b and c used in eq. (1) are determined as given below:

$$\begin{aligned} a &= \sqrt{(\epsilon_{y,\theta} - \epsilon_{p,\theta}) (\epsilon_{y,\theta} - \epsilon_{p,\theta} + c/E_\theta)}, \\ b &= \sqrt{c (\epsilon_{y,\theta} - \epsilon_{p,\theta}) E_\theta + c^2}, \\ c &= \frac{(f_{y,\theta} - f_{p,\theta})^2}{(\epsilon_{y,\theta} - \epsilon_{p,\theta}) E_\theta - 2(f_{y,\theta} - f_{p,\theta})}. \end{aligned} \quad (2)$$

Fig. 1 (a) shows that the elevated temperature effective yield strength $f_{y,\theta}$ and proportional limit $f_{p,\theta}$ are calculated by multiplying the elevated temperature yield strength reduction factor $k_{y,\theta}$ and proportional limit reduction factor $k_{p,\theta}$ by the room temperature yield strength f_y (i.e. $f_{y,\theta} = k_{y,\theta} f_y$ and $f_{p,\theta} = k_{p,\theta} f_y$). On the other hand, the elevated temperature Young's modulus E_θ is calculated by multiplying the elevated temperature Young's modulus reduction factor $k_{E,\theta}$ by the room temperature Young's modulus of carbon steel E (i.e. $E_\theta = k_{E,\theta} E$). In this paper, the values of $k_{y,\theta}$, $k_{p,\theta}$ and $k_{E,\theta}$ provided in EN 1993-1-2 [28], which are displayed in Fig. 1 (b), were employed for grade S355, S275 and S235 steels. Note that $k_{p0.2,\theta}$ is the elevated temperature 0.2% proof strength reduction factor multiplied by the yield strength f_y to determine the elevated temperature 0.2% proof strength $f_{p0.2,\theta}$ (i.e. $f_{p0.2,\theta} = k_{p0.2,\theta} f_y$).

The EN 1993-1-2 [28] elevated temperature material model given by eq. (1) was originally developed by Rubert and Schaumann [44] on the basis of the findings of a series of anisothermal tests carried out on normal strength steel beams, resulting in an accurate representation of the elevated temperature material response of normal strength steels. However, previous research studies [45–47] demonstrated that the EN 1993-1-2 [28] elevated temperature material model leads to unconservative estimations of the elevated temperature stress-strain response of high strength steels; thus, its use to define the elevated temperature material

behaviour of high strength steels may lead to unconservative predictions of the resistances of high strength steel elements at elevated temperatures. Thus, the EN 1993-1-2 [28] elevated temperature material model was only used for normal strength grade S355, S275 and S235 steel plates in this paper. In the case of high strength grade S690 and S460 steel plates, the two-stage elevated temperature material model proposed in Fang and Chan [12, 13] for high strength grade S690 and S460 steels, based on the elevated temperature material model for high strength steels recommended by Chen and Young [11], was adopted. This material model is defined through the following equations:

$$\begin{aligned} \epsilon &= \frac{\sigma}{E_\theta} + 0.002 \left(\frac{\sigma}{f_{p0.2,\theta}} \right)^{n_\theta} & \text{for } \sigma \leq f_{p0.2,\theta}, \\ \epsilon &= \frac{\sigma - f_{p0.2,\theta}}{E_{p0.2,\theta}} + \epsilon_{u,\theta} \left(\frac{\sigma - f_{p0.2,\theta}}{f_{u,\theta} - f_{p0.2,\theta}} \right)^{m_\theta} + \epsilon_{p0.2,\theta} & \text{for } f_{p0.2,\theta} \leq \sigma \leq f_{u,\theta}, \end{aligned} \quad (3)$$

where $\epsilon_{p0.2,\theta}$ is the total strain corresponding to $f_{p0.2,\theta}$, n_θ and m_θ are the exponents defining the roundedness of the stress-strain curve and $E_{p0.2,\theta}$ is the tangent modulus at $f_{p0.2,\theta}$, which is calculated by

$$E_{p0.2,\theta} = \frac{E_\theta}{(1 + 0.002n_\theta E_\theta / f_{0.2p,\theta})}. \quad (4)$$

The exponents n_θ and m_θ can be determined using the following expressions for grade S690 steel [13]:

$$\begin{aligned} n_\theta &= 7 - \frac{\theta}{250}, \\ m_\theta &= 1.6 + \frac{\theta}{600}, \end{aligned} \quad (5)$$

and the following equations for grade S460 steel [12, 13]:

$$\begin{aligned} n_\theta &= 12 - \frac{\theta}{100}, \\ m_\theta &= 2.1 + \frac{3\theta}{600}. \end{aligned} \quad (6)$$

It is worth noting that in [11–13], the elevated temperature material model given by eq. (3) was developed taking into account the two-stage compound Ramberg-Osgood material model proposed by Mirambell and Real [48] for the representation of the stress-strain response of stainless steels at room temperature; Fang and Chan [12, 13] and Chen and Young [11] demonstrated that this material model furnishes accurate predictions of the stress-strain response of high strength steels at elevated temperatures with appropriate n_θ and m_θ exponents used to define the roundedness of the stress-strain curves.

In the finite element models of high strength steel plates created in this study, the elevated temperature material properties (i.e. E_θ , $f_{p0.2,\theta}$, $f_{y,\theta}$, $f_{u,\theta}$ and $\epsilon_{u,\theta}$) of grade S690

and S460 steels determined through the elevated temperature material tests performed on high strength grade S690 and S460 steels by Qiang et al. [49] and Qiang et al. [50] were utilised. The room temperature yield strength f_y , ultimate tensile strength f_u and strain ϵ_u and the Young's modulus E for grade S690 and S460 steels determined through the room temperature material tests in [49, 50] were multiplied by the material reduction factors (i.e. $k_{E,\theta}$, $k_{p0.2,\theta}$, $k_{y,\theta}$ and $k_{u,\theta}$) derived in [49, 50] to determine their values at corresponding elevated temperature levels θ in this paper, i.e. $E_\theta = k_{E,\theta}E$, $f_{p0.2,\theta} = k_{p0.2,\theta}f_y$, $f_{y,\theta} = k_{y,\theta}f_y$, $f_{u,\theta} = k_{u,\theta}f_u$ and $\epsilon_{u,\theta} = k_{\epsilon_{u,\theta}}\epsilon_u$. Therefore, the room temperature material properties of grade S690 steel were taken as $E = 204690$ MPa, $f_y=789$ MPa, $\sigma_u=821$ MPa and $\epsilon_u=0.051$ as obtained in [49], while those of grade S460 steel were taken as $E = 202812$ MPa, $f_y=504$ MPa, $\sigma_u=640$ MPa and $\epsilon_u=0.115$ as determined in [50]. Table 1 and Table 2 display the corresponding material reduction factors for S690 and S460 steels provided in [49, 50] adopted in this study as well as the Ramberg-Osgood parameters n_θ and m_θ determined through eq. (5) and eq. (6) for different elevated temperature levels. Note that the elevated temperature 0.2% proof strength reduction factors $k_{p0.2,\theta}$ for grade S460 steel and the reduction factors for strains corresponding to the elevated temperature ultimate strengths $k_{\epsilon_{u,\theta}}$ presented in Table 1 and Table 2 were obtained from the corresponding experimental stress-strain curves provided in [49–51]. In Fig. 2, the Young's modulus $k_{E,\theta}$ and yield strength reduction factors $k_{y,\theta}$ used for high strength grade S690 and S460 steels against those adopted for normal strength grade S355, S275 and S235 steels are shown, indicating that while the yield strength reduction $k_{y,\theta}$ for grade S690 and S460 steels is both less severe than that for normal strength steels, the Young's modulus reduction is less severe for grade S690 steel but more pronounced for grade S460 steel relative to that for normal strength steels. Fig. 3 illustrates comparison of the elevated temperature stress-strain response of grade S690 and S460 steels obtained using eq. (3) and the elevated temperature material properties from [49, 50] against the elevated temperature stress-strain curves determined through the material tests by [49, 50]. As can be seen from the figures, the stress-strain curves adopted in the finite element models are in close agreement with those obtained from the material tests by [49, 50].

2.3. Boundary conditions

Fig. 4 shows the adopted boundary conditions within the finite element models of internal elements and outstand flanges. As can be seen from the figure, to replicate simply-supported boundary conditions, only the vertical translations $U3$ of the longitudinal edges were restrained (i.e. $U3 = 0$). In the case of the loaded edges of the plates, the vertical translations $U3$ were also restrained as well as the horizontal translations $U2$ at the mid-width nodes (i.e. $U2 = 0$), thereby establishing simply-supported conditions for the loaded edges. Additionally, the translation of the mid-width node of the one of the loaded edges was also restrained in the longitudinal direction (i.e. $U1 = 0$). For the purpose of avoiding localised yielding, the loaded edges were constrained to the mid-width nodes where the loads were applied as point forces or moments. The appropriateness of the boundary and loading conditions was carefully verified by comparing the elastic critical buckling stresses obtained through the Linear Buckling Analyses (LBA) of the finite element models against

those obtained from the formulae provided in [33–35]. There was a very good agreement between the elastic critical stresses obtained through the finite element models and those determined analytically, thus verifying that the adopted boundary and loading conditions in the numerical simulations were appropriate.

2.4. Initial imperfections

The presence of local geometric imperfections can lead to considerable reductions in the ultimate strengths of steel plates in fire. In the finite element models, the local imperfections were modelled by adopting the lowest local buckling modes obtained through the Linear Buckling Analyses (LBA) of steel plates as shown in Fig. 5. These local buckling mode shapes were scaled to 1/200 of the plate widths b (i.e. $e_0 = b/200$) for internal plate elements, while they were scaled to 1/50 of the plate widths b for outstand flanges (i.e. $e_0 = b/50$) in line with the recommendations given in EN 1993-1-5 [52].

2.5. Validation of finite element models

The finite element modelling approach adopted in this study is validated against the results obtained from the isothermal fire experiments carried out on a series of stub columns by Pauli et al. [18] and Wang et al. [20]. In the experiments of Pauli et al. [18], grade S355 steel square hollow section (SHS) stub columns were used, while grade S235 normal strength and grade S460 high strength steel welded I-section stub columns were tested in Wang et al. [20]. Cross-section properties of the specimens reported in [18, 20] were used in the finite element models. Local imperfections were applied to the models as described in Section 2.4. The elevated temperature material properties of the specimens were defined using the elevated temperature material models and reduction factors provided in Section 2.2 for grade S235 and S355 normal strength and grade S460 high strength steels, considering the room temperature material properties of the specimens provided in [18, 20]. In the validation study carried out herein, (i) the finite element model of a critical plate (internal element or outstand flange) of a stub column with the lowest elastic critical buckling stress (relative to those of all the constituent plates) was created and (ii) the numerical failure load of the stub column $N_{u,FE}$ was determined by considering the failure load of the critical plate $N_{u,FE,plate}$ and the corresponding cross-section area of the critical plate A_{plate} and stub column A_{stub} (i.e. $N_{u,FE} = (N_{u,FE,plate}/A_{plate})A_{stub}$), i.e. it was assumed that the ultimate load carrying capacity of the stub column section is achieved with the failure of the most critical plate. Note that this approach was adopted in the validation of the finite element models of steel plates since there are no fire tests performed on individual steel plates in the literature.

In Table 3, the failure loads of grade S235 normal strength and grade S460 high strength steel I-section stub columns obtained from the fire experiments of Wang et al. [20] and the finite element models created herein are compared. Note that the welded I-sections of the specimens of [20] are denoted as I- $h \times b \times t_w \times t_f$ in the table, where h and b are the cross-section depth and width and t_w and t_f are the web and flange thicknesses, respectively. The failure loads of the specimens determined in the experiments and through the developed finite element models at room temperature are also included in the table for comparison. As indicated in Table 3, Wang et al. [20] specified the cross-section dimensions of the stub

columns such that either the outstand flanges or internal elements were the critical plates. Table 3 shows that the finite element models provide failure loads that are generally in a good agreement with those observed in the experiments of normal strength and high strength steel stub columns for both internal element and outstand flange critical cases. The differences in the experimental and numerical failure loads were ascribed to differences in the shapes and magnitudes of the geometric imperfections of the specimens and those adopted in the finite element models and the difficulties in controlling the fire tests for the specimens heated by more than 600 °C. The failure loads of the grade S355 normal strength steel square hollow section (SHS) stub columns with cross-section width of 160 mm and thickness of 5 mm (i.e. SHS 160 × 160 × 5) obtained from the experiments performed in Pauli et al. [18] are compared against those determined through the finite element models created in this study in Table 4. As can be seen from Table 4, there is generally a good correlation between the experimental and numerical failure loads. Since the finite element models created in this study provide very accurate predictions of the elastic critical buckling stresses of steel plates and they are also able to provide accurate estimations of the ultimate strengths of normal strength and high strength steel stub columns in fire, it was assumed that they are able to replicate the behaviour of steel plates at elevated temperatures accurately.

2.6. Parametric studies

Summary of the numerical parametric studies carried out in this paper is provided in Table 5. As can be seen from the table, the loading and boundary conditions corresponding to internal elements under compression, internal elements under bending and outstand flanges under compression were taken into consideration. For each considered plate type and loading condition, the high strength steel grades of S690, S460 as well as the normal strength steel grades of S355, S275 and S235 were considered. Five elevated temperature levels equal to 300 °C, 400 °C, 500 °C, 600 °C and 700 °C were accounted for. To explore a broad spectrum of plate buckling response at elevated temperatures, nineteen plate slendernesses $\bar{\lambda}_p$ equal to the square root of the ratio of the room temperature yield stress f_y to the elastic critical plate buckling stress σ_{cr} (i.e. $\bar{\lambda}_p = \sqrt{f_y/\sigma_{cr}}$) ranging between 0.2 and 2.0 with increment in $\bar{\lambda}_p$ of 0.1 were taken into account (i.e. $\bar{\lambda}_p = [0.2, 2.0]$ with $\Delta\bar{\lambda}_p = 0.1$). In total, 1425 plates were taken into consideration in the parametric studies.

In the following sections, the structural performance data obtained from the parametric studies will be used to assess the accuracy of the methods provided in EN 1993-1-2 [28] and prEN 1993-1-2 [30] and in the development of a new effective width method for the local buckling strength predictions of normal strength and high strength steel plates in fire. Prior to this, it is worthwhile investigating the influence of residual stresses on the local buckling strengths of steel plates. Fig. 6 shows the influence of residual stresses on the ultimate resistances of high strength and normal strength steel internal elements and outstand flanges at elevated temperatures, where $R_{GMNIA,no,res}$ and $R_{GMNIA,res}$ are the ultimate resistances obtained considering and neglecting residual stresses, respectively. In Fig. 6, the elevated temperature values of 300 °C, 400 °C, 500 °C, 600 °C and 700 °C and plate slenderness values $\bar{\lambda}_p$ ranging between 0.2 and 2.0 with increment in $\bar{\lambda}_p$ of 0.1 were taken into consideration for each high strength and normal strength steel grade. Note that the residual stress pattern

recommended by Bradford et al. [53] for welded high strength steel sections was incorporated into the finite element models of grade S690 and S460 high strength steel plates. For the case of steel plates with residual stresses whose results are presented in Fig. 6, the numerical models were analysed isothermally by adopting the following steps: (i) application of the residual stresses to the numerical models at room temperature, (ii) application of a uniform temperature increase to the models incrementally from room temperature to a predefined temperature value θ which results in the development of thermal strains in the models as well as the modification of their material response and finally, (iii) application of the loading to the numerical models at the designated elevated temperature level θ . As can be seen from Fig. 6, the influence of residual stresses on the ultimate resistances of both high strength and normal strength steel plates is rather low at elevated temperatures. On the basis of this observation, residual stresses were not incorporated into the finite element models of steel plates in this study, which was in accordance with Quiel and Garlock [22] and Couto et al. [25] where the residual stresses were also not included in the numerical models considering their low influence on the ultimate resistances of steel plates in fire.

3. EN 1993-1-2 and prEN 1993-1-2 design approaches for the local buckling assessment of normal and high strength steel elements at elevated temperatures

In this section, the cross-section classification approach and effective width design rules provided in EN 1993-1-2 [28] and its upcoming version prEN 1993-1-2 [30] are briefly set out. Afterwards, the accuracy of EN 1993-1-2 [28] and prEN 1993-1-2 [30] is investigated for the determination of ultimate resistances of normal and high strength steel plates in fire.

3.1. Cross-section classification

Both EN 1993-1-2 [28] and prEN 1993-1-2 [30] recommend the use of the cross-section classification rules provided in the room temperature European structural steel design standard EN 1993-1-1 [54] and its upcoming version prEN 1993-1-1 [55] respectively in conjunction with a reduced value for material factor ϵ_θ , which is determined as

$$\epsilon_\theta = 0.85\epsilon = 0.85\sqrt{235/f_y} \quad \text{where } f_y \text{ in MPa,} \quad (7)$$

where ϵ is the room temperature material factor. In EN 1993-1-1 [54] and prEN 1993-1-1 [55], steel sections are categorised into four classes, where the cross-section class is assumed as the highest class of its constituent plates. The limit width-to-thickness ratios provided in Table 6 are utilised to specify the classes of the internal and outstand elements of cross-sections. Note that 0.85 reduction factor, applied to the room temperature material factor ϵ for the determination of the elevated temperature material factor ϵ_θ , is used to approximate the values of the square root of the ratios of the stiffness reduction factors $k_{E,\theta}$ to the yield strength reduction factors $k_{y,\theta}$ (i.e. $\sqrt{k_{E,\theta}/k_{y,\theta}}$) as shown in Fig. 7, i.e. $\sqrt{k_{E,\theta}/k_{y,\theta}} \approx 0.85$ and $\epsilon_\theta = \left(\sqrt{k_{E,\theta}/k_{y,\theta}}\right)\epsilon \approx 0.85\epsilon$. However, as can be seen from the figure, 0.85 factor somewhat underestimates the values of $\sqrt{k_{E,\theta}/k_{y,\theta}}$ for high strength steel grade of S690. Moreover,

this type of cross-section classification approach also neglects the differential erosions of the strengths and stiffnesses at different elevated temperature levels shown in Fig. 7, which considerably influence the local buckling response of steel elements in fire.

3.2. Effective width method

Thin-walled steel plates subjected to in-plane compressive stresses are able to exhibit significant post-ultimate strengths, where their ultimate load carrying capacities can go well beyond their elastic critical buckling loads with the development of non-uniform stresses across the plate widths. As shown in Fig. 8, the effective width method adopted in EN 1993-1-2 [28] and prEN 1993-1-2 [30] accounts for the post-ultimate strengths of steel plates, representing the non-uniform stress distributions by means of uniform stress blocks with effective widths of b_{eff} . In the effective width method, the effective widths of the uniform stress blocks are determined as

$$b_{eff} = \rho b, \quad (8)$$

in which ρ is the plate buckling reduction factor. EN 1993-1-2 [28] recommends the use of the effective width formulations provided in the room temperature structural steel design standard EN 1993-1-5 [28] for the determination of the plate buckling reduction factor. The plate buckling reduction factor ρ is determined for internal elements according to EN 1993-1-5 [52] as:

$$\rho = \begin{cases} 1.0 & \text{for } \bar{\lambda}_p \leq 0.5 + \sqrt{0.085 - 0.055\psi}, \\ \frac{\bar{\lambda}_p - 0.055(3 + \psi)}{\bar{\lambda}_p^2} \leq 1.0 & \text{for } \bar{\lambda}_p > 0.5 + \sqrt{0.085 - 0.055\psi}, \end{cases} \quad (9)$$

where ψ is the ratio of the stresses at the edges of the plate. On the other hand, ρ is determined for outstand flanges as follows:

$$\rho = \begin{cases} 1.0 & \text{for } \bar{\lambda}_p \leq 0.748, \\ \frac{\bar{\lambda}_p - 0.188}{\bar{\lambda}_p^2} \leq 1.0 & \text{for } \bar{\lambda}_p > 0.748. \end{cases} \quad (10)$$

In eq. (9) and eq. (10), $\bar{\lambda}_p$ is the non-dimensional plate slenderness equal to:

$$\bar{\lambda}_p = \sqrt{\frac{f_y}{\sigma_{cr}}} = \frac{b/t}{28.4\epsilon\sqrt{k_\sigma}} \quad (11)$$

in which σ_{cr} is the elastic critical buckling stress of the plate, k_σ is the buckling coefficient calculated on the basis the stress distribution and edge boundary conditions and t is the plate thickness.

Different than EN 1993-1-2 [28], the upcoming version of the European structural steel fire design standard prEN 1993-1-2 [30] does not direct the designer to another standard but

provides equations for the determination of plate buckling reduction factors ρ . According to prEN 1993-1-2 [30], the buckling reduction factor ρ is determined for internal elements as:

$$\rho = \frac{(\bar{\lambda}_p + 0.9 - 0.26/\epsilon)^{1.5} - 0.055(3 + \psi)}{(\bar{\lambda}_p + 0.9 - 0.26/\epsilon)^3} \leq 1.0, \quad (12)$$

and for outstand flanges as:

$$\rho = \frac{(\bar{\lambda}_p + 1.1 - 0.52/\epsilon)^{1.2} - 0.188}{(\bar{\lambda}_p + 1.1 - 0.52/\epsilon)^{2.4}} \leq 1.0, \quad (13)$$

where ϵ is the material factor equal to $\epsilon = \sqrt{235/f_y}$ as previously introduced. As can be understood from the design formulae provided in this subsection, the effective width equations provided in both EN 1993-1-2 [28] and prEN 1993-1-2 [55] do not account for the differential erosions of strengths and stiffnesses of steel plates during buckling at elevated temperatures, whose influence can be significant for the response, and simply use the room temperature plate slendernesses $\bar{\lambda}_p$ for the determination of the ultimate resistances of steel plates in fire.

3.3. Cross-section resistance

EN 1993-1-2 [28] and prEN 1993-1-2 [55] recommend the determination of the cross-section resistances considering the cross-section class as shown in Table 7, in which $N_{fi,t,Rd}$ and $M_{fi,t,Rd}$ are the axial force and bending moment design resistances in fire at time t , A and A_{eff} are the gross and effective cross-section areas, W_{pl} , W_{el} and W_{eff} are the plastic, elastic and effective section moduli respectively and $\gamma_{M,fi}$ is the partial factor for fire design. As can be seen from Table 7, both EN 1993-1-2 [28] and prEN 1993-1-2 [55] adopt the approach provided in the room temperature design standards EN 1993-1-1 [54] and prEN 1993-1-1 [55] for the determination of the cross-section resistances of sections falling into particular classes, using the elevated temperature material strengths (i.e. $f_{y,\theta} = k_{y,\theta}f_y$ and $f_{p0.2,\theta} = k_{p0.2,\theta}f_y$). However, while EN 1993-1-2 [28] recommends the use of the elevated temperature 0.2% proof strength $f_{p0.2,\theta} = k_{p0.2,\theta}f_y$ for Class 4 sections, prEN 1993-1-2 [30] recommends the cross-section resistances of Class 4 sections to be determined using the elevated temperature strength at 2% total strain $f_{y,\theta} = k_{y,\theta}f_y$.

3.4. Assessment of the accuracy of EN 1993-1-2 and prEN 1993-1-2 design approaches for the local buckling assessment of normal and high strength steel plates in fire

In this subsection, the accuracy of EN 1993-1-2 [28] and prEN 1993-1-2 [30] is assessed for the determination of the resistances of normal and high strength steel plates at elevated temperatures. Fig. 9 shows the accuracy of EN 1993-1-2 [28] in the predictions of the ultimate strengths of grade S690 and S460 high strength and grade S355 and S235 normal strength steel internal elements subjected to compression in fire. As can be seen from the figure, the existing effective width equations given in EN 1993-1-2 [28], which neglect the differential erosions of the strengths and stiffnesses at elevated temperatures, lead to rather

unconservative and inaccurate ultimate strength predictions for internal steel elements under compression. Owing to the adoption of the elevated temperature strengths at 2% total strain $f_{y,\theta} = k_{y,\theta}f_y$ for Class 1, 2 and 3 sections and 0.2% proof strengths $f_{p0.2,\theta} = k_{p0.2,\theta}f_y$ for Class 4 sections, there are also abrupt changes in the ultimate strength predictions determined through EN 1993-1-2 [28] at the transitions between Class 3 and Class 4 sections according to the cross-section classification limits given in Table 6 with the elevated temperature material factor ϵ_θ . Note that even though EN 1993-1-2 [28] adopts a single plate buckling curve, the ordinates of the ultimate strength predictions determined using EN 1993-1-2 [28] shown in Fig. 9 for Class 4 plates vary at different elevated temperatures levels due to (i) the determination of the resistances of Class 4 sections using the elevated temperature 0.2% proof strengths $f_{p0.2,\theta} = k_{p0.2,\theta}f_y$ and (ii) different ratios between the elevated temperature 0.2% proof strengths $f_{p0.2,\theta} = k_{p0.2,\theta}f_y$ and the elevated temperature strengths at 2% total strains $f_{y,\theta} = k_{y,\theta}f_y$ (i.e. $f_{p0.2,\theta}/f_{y,\theta} = k_{p0.2,\theta}/k_{y,\theta}$) at different elevated temperature levels. It is also noteworthy that since, in some cases, the elevated temperature 0.2% proof strengths $f_{p0.2\theta}$ of grade S690 and S460 high strength steels are greater than their elevated temperature strengths at 2% total strains $f_{y,\theta}$ (i.e. $f_{p0.2\theta} > f_{y,\theta}$), which is due to the latter being in the descending branches of the stress-strain curves (see Fig. 3, Table 1 and Table 2), there exist increases in the ultimate resistance predictions determined according to EN 1993-1-2 [28] for grade S690 and S460 high strength steel internal elements at the transitions between Class 3 and Class 4 plates. This, of course, does not at all represent the physical reality of the actual behaviour of these high strength steel plates at elevated temperatures.

In Fig. 9, the accuracy of the revised effective width design equations provided in the upcoming version of the European structural steel fire design standard prEN 1993-1-2 [28] is also assessed. As can be seen from the figure, prEN 1993-1-2 [28] leads to an improved level of accuracy relative to EN 1993-1-2 [28] in the determination of the ultimate resistances of grade S355 and S235 normal strength steel plates at elevated temperatures, where there are no variations in the ordinates of the ultimate resistance predictions at different elevated temperature levels owing to the adoption of the elevated temperature strengths at 2% total strain $f_{y,\theta} = k_{y,\theta}f_y$ for all Class 1, 2, 3 and 4 sections. However, for the case of high strength steel plates, prEN 1993-1-2 [28] effective width equations, which were originally developed for normal strength steel elements, lead to significant underestimations of the ultimate resistances, thus leading to uneconomic designs. Moreover, similar to EN 1993-1-2 [28], prEN 1993-1-2 [30] also leads to significant overpredictions of the ultimate strengths of moderately slender plates with plate slendernesses varying between 0.2 and 0.6 (i.e. $0.2 < \bar{\lambda}_p < 0.6$). This was attributed to the adoption of the room temperature cross-section classification limits given in prEN 1993-1-1 [55], which are shown in Table 6, with the elevated temperature material factors $\epsilon_\theta = 0.85\epsilon = 0.85\sqrt{235/f_y}$ by prEN 1993-1-2 [30]. Note that even though $\epsilon_\theta = 0.85\epsilon$ leads to a conservative estimation of $\epsilon_\theta = \sqrt{k_{E,\theta}/k_{y,\theta}}\epsilon$ (see Fig. 7), the use of $\epsilon_\theta = 0.85\epsilon$ with the room temperature cross-section classification rules provided in prEN1993-1-2 [55] does not take into account significantly more nonlinear stress-strain response of steels at elevated temperatures relative to that at room temperature, which leads to earlier loss of stiffness due to earlier plastification and thus lower ultimate

strengths. The effective width design formulae given in prEN 1993-1-2 [30] provide plate buckling coefficients ρ lower than 1.0 (i.e. $\rho < 1.0$) for non-Class 4 plates according to the cross-section classification approach provided prEN 1993-1-2 [30]; this highlights that there exists an incompatibility between the effective width design equations and cross-section classification approach given in prEN 1993-1-2 [30], resulting in unconservative strength estimations for non-Class 4 plates. This is also the reason behind the discontinuities in the ultimate strength predictions of prEN 1993-1-2 [28] at the transitions between Class 3 and Class 4 plates as shown in Fig. 9 since the plate buckling coefficients ρ are already considerably smaller than unity (i.e. $\rho < 1.0$) for the corresponding slendernesses $\bar{\lambda}_p$ at the transitions of the plates from Class 3 to Class 4 category.

It is worth noting that as can be seen in Fig. 9, the ultimate resistances of grade S690 and S460 high strength steel plates exhibit a higher level of scatter at different temperature levels relative to those of grade S355 and S235 normal strength steel plates. This was ascribed to (i) the variation of the roundedness of the elevated temperature stress-strain curves of high strength steels at different elevated temperature levels adopting varying n_θ and m_θ exponents and (ii) the use of the elevated temperature strength at 2% total strain $f_{y,\theta}$ in the normalisation of the resistances of high strength steel plates, despite the ultimate strains $\epsilon_{u,\theta}$ corresponding to the elevated temperature ultimate material strengths $f_{u,\theta} = k_{u,\theta} f_u$ being lower than 2% (i.e. $\epsilon_{u,\theta} < 0.02$) for grade S690 and S460 steels as shown in Fig. 3 in some instances. Considering that, in some cases, the elevated temperature strengths at 2% total strains $f_{y,\theta}$ are located within the descending branches of the elevated temperature stress-strain curves (see Fig. 3) due to the lower ductility of high strength steels, it could be argued that the use of the elevated temperature strengths at 2% strengths $f_{y,\theta} = k_{y,\theta} f_y$ may not be suitable in the determination of the ultimate resistances of grade S690 and S460 high strength steel plates in these cases.

The accuracy of EN 1993-1-2 [28] and prEN 1993-1-2 [30] is also assessed in Fig. 10 for high strength and normal strength internal elements under bending, considering the high strength grades of S690 and S460 and the normal strength grades of S355 and S235. Note that owing to the determination of ultimate resistances of Class 1 and 2 sections using plastic section modulus W_{pl} and the calculation of ultimate resistances of Class 3 sections using elastic section modulus W_{el} , there exist two plateaus in the plate buckling curves of EN 1993-1-2 [28] and prEN 1993-1-2 [30] for Class 1 and 2 and Class 3 plates. As can be seen in Fig. 10, similar to the predictions for internal elements under compression, EN 1993-1-2 [28] also leads to unconservative estimations of the elevated temperature ultimate resistances of internal elements under bending. However, the overestimations are lower in this loading case. Fig. 10 also shows that the new design equations given in prEN 1993-1-2 [30] lead to an improved level of safety relative to EN 1993-1-2 [28]. However, again, the new effective width equations provided in prEN 1993-1-2 [30] result in considerable underestimations of the ultimate strengths of grade S690 and S460 high strength steel internal elements under bending. Moreover, there still exist significant overestimations for the Class 2 and 3 plates by prEN 1993-1-2 [30] due to the adoption of the room temperature cross-section classification limits provided in prEN 1993-1-1 [55] with the elevated temperature material factors $\epsilon_\theta = 0.85\epsilon$ even though the plate buckling reduction factors ρ determined through

the effective width equations of [55] are lower than 1.0 for these cases (i.e. $\rho < 1.0$), so again highlighting the incompatibility between the cross-section classification limits and effective width equations provided in prEN 1993-1-2 [55].

Finally, the accuracy of EN 1993-1-2 [28] and prEN 1993-1-2 [30] is assessed for grade S690 and S460 high strength and grade S355 and S275 normal strength steel outstand flanges under compression in Fig. 11. As can be seen in the figure, EN 1993-1-2 [28] leads to rather inaccurate estimations of the ultimate resistances of high strength and normal strength steel outstand plates under compression at elevated temperatures. Relative to EN 1993-1-2 [28], prEN 1993-1-2 [30] provides strength predictions with higher accuracy, though they are still overly-conservative for high strength steel plates, indicating that new effective width design equations leading to accurate ultimate resistance estimations of both high strength and normal strength steel outstand flanges under compression is necessary. Note that the lower accuracy of the local buckling assessment provisions provided in EN 1993-1-2 [28] and prEN1993-1-1 [55] for high strength steels is also associated with the use of different elevated temperature stress-strain response for high strength steels relative to that used for normal strength steels in this study, which are shown to provide a considerably more accurate representation of the elevated temperature material response of high strength steels in comparison to the EN 1993-1-2 [28] elevated temperature material model [12, 13].

4. New cross-section classification approach and effective width design method for normal strength and high strength steel elements in fire

With the aim of achieving accurate and safe estimations of the ultimate strengths of both high strength and normal strength steel elements at elevated temperatures, new cross-section classification rules and effective width equations are put forward in this section. In the following section, the accuracy of the proposed design rules for the predictions of the ultimate resistances of grade S690 and S460 high strength steel and grade S355, S275 and S235 normal strength steel plates are investigated.

4.1. New cross-section classification approach

In line with the cross-section classification approach put forward in Couto et al. [25] and Xing et al. [32], in this study, it is proposed to replace the traditional four cross-section classes used in the room temperature design with two classes referred to as ‘non-slender’ and ‘slender’ for the determination of the ultimate strengths of high strength and normal strength steel cross-sections in fire. In this cross-section classification approach, a cross-section is classified as ‘non-slender’ only if all of its constituent plates are classified as ‘non-slender’, while if one or more constituent plates of a section is classified as ‘slender’, the section is classified as ‘slender’. Individual constituent plates of a cross-section is classified by comparing their elevated temperature plate slendernesses $\bar{\lambda}_{p,\theta}$ against the plateau plate slendernesses given by eq. (15) and eq. (17). If the elevated temperature slenderness of a constituent plate $\bar{\lambda}_{p,\theta}$ is less than or equal to the plateau slenderness $\bar{\lambda}_{p,\theta,0}$ (i.e. $\bar{\lambda}_{p,\theta} \leq \bar{\lambda}_{p,\theta,0}$), the plate is classified as ‘non-slender’. On the other hand, if the plate slenderness $\bar{\lambda}_{p,\theta}$ is larger than the plateau slenderness (i.e. $\bar{\lambda}_{p,\theta} > \bar{\lambda}_{p,\theta,0}$), the plate is classified as ‘slender’. In

the classification of the internal elements and outstand flanges, the corresponding plateau slendernesses provided in eq. (15) for internal elements and eq. (17) for outstand flanges are taken into consideration.

4.2. New effective width method for normal and high strength steel plates in fire

To account for differential erosions of strengths and stiffnesses of steel plates on their local buckling response at elevated temperatures, in the new effective width equations, the elevated temperature plate slendernesses $\bar{\lambda}_{p,\theta}$ were used, adopting the format of the effective width equations provided in EN 1993-1-5 [28].

For internal elements, the following equations are proposed for the determination of the local buckling reduction factor ρ of both high strength and normal strength plates:

$$\rho = \begin{cases} 1.0 & \text{for } \bar{\lambda}_{p,\theta} \leq \bar{\lambda}_{p,\theta,0}, \\ \frac{0.9 - 0.38\epsilon}{\bar{\lambda}_{p,\theta}^{0.85}} - \frac{0.015(3 + \psi)}{\bar{\lambda}_{p,\theta}^{1.7}} & \text{for } \bar{\lambda}_{p,\theta} > \bar{\lambda}_{p,\theta,0} \end{cases} \quad (14)$$

with

$$\bar{\lambda}_{p,\theta,0} = \left(0.45 - 0.19\epsilon + \sqrt{\frac{(0.9 - 0.38\epsilon)^2}{4} - 0.015(3 + \psi)} \right)^{1.18}, \quad (15)$$

where ψ is the ratio between the stresses at the edges of the plate as described in EN 1993-1-5 [52] and ϵ is the material factor equal to $\epsilon = \sqrt{235/f_y}$.

For outstand flanges, the proposed plate buckling reduction factors ρ are calculated as follows:

$$\rho = \begin{cases} 1.0 & \text{for } \bar{\lambda}_{p,\theta} \leq \bar{\lambda}_{p,\theta,0}, \\ \frac{0.9 - 0.3\epsilon}{\bar{\lambda}_{p,\theta}^{0.6}} - \frac{0.05}{\bar{\lambda}_{p,\theta}^{1.2}} & \text{for } \bar{\lambda}_{p,\theta} > \bar{\lambda}_{p,\theta,0} \end{cases} \quad (16)$$

with

$$\bar{\lambda}_{p,\theta,0} = \left(0.45 - 0.15\epsilon + \sqrt{\frac{(0.9 - 0.3\epsilon)^2}{4} - 0.05} \right)^{1.67}. \quad (17)$$

In eq. (14) and eq. (16), $\bar{\lambda}_{p,\theta,0}$ is the threshold plate slenderness and $\bar{\lambda}_{p,\theta}$ is the elevated temperature plate slenderness determined as:

$$\bar{\lambda}_{p,\theta} = \xi_\theta \sqrt{\frac{f_y}{\sigma_{cr}}} \quad \text{with} \quad \xi_\theta = \sqrt{\frac{k_{y,\theta}^*}{k_{E,\theta}}}, \quad (18)$$

in which f_y is the room temperature yield strength and σ_{cr} is the elastic critical buckling stress calculated using the following equation:

$$\sigma_{cr} = k_\sigma \frac{\pi^2 E}{12(1 - \nu^2)} \left(\frac{t}{b} \right)^2, \quad (19)$$

where k_σ is the plate buckling coefficient determined considering the boundary conditions and stress distribution of the plate as described in EN 1993-1-5 [52], ν is the Poisson's ratio and b and t are the plate width and thickness, respectively.

In eq. (18), $k_{y,\theta}^*$ is the modified elevated temperature yield strength reduction factor calculated as follows:

$$k_{y,\theta}^* = k_{y,\theta} \quad \text{if } k_{\epsilon_{u,\theta}} \epsilon_{u,\theta} \geq 0.02, \quad (20)$$

$$k_{y,\theta}^* = k_{u,\theta} \frac{f_u}{f_y} \quad \text{if } k_{\epsilon_{u,\theta}} \epsilon_{u,\theta} < 0.02. \quad (21)$$

The use of the modified elevated temperature yield strength reduction factors $k_{y,\theta}^*$ in the effective width design equations and in the determination of the cross-section resistances as described in the following subsection precludes the use of the elevated temperature material strengths at 2% total strains (i.e. $f_{y,\theta} = k_{y,\theta} f_y$) when the strains corresponding to the elevated temperature ultimate strengths $\epsilon_{u,\theta} = k_{\epsilon_{u,\theta}} \epsilon_u$ are smaller than 2% (i.e. $\epsilon_{u,\theta} < 0.02$), which is observed for high strength steels at some elevated temperature levels owing to their low ductility (see Fig. 3). This avoids the use of the material strengths within the descending branches of the elevated temperature stress-strain curves and enables the use of the elevated temperature ultimate strengths $f_{u,\theta} = k_{u,\theta} f_u$ in the estimations of the ultimate resistances of high strength steel plates in fire in these cases. In Kucukler [37], this approach was utilised in the determination of the ultimate strengths of high strength steel circular hollow section (CHS) members under compression in fire, which was shown to enable accurate estimations of their ultimate resistances.

4.3. Cross-section resistance

In Table 8, the estimations of the cross-section resistances of cross-sections falling into the non-slender and slender classes according to the proposed cross-section classification approach is illustrated. For the case of cross-sections falling into the non-slender class, the utilisation of the full cross-section areas A and the plastic section moduli W_{pl} is proposed. On the other hand, for the case of cross-sections falling into the slender class, the use of the effective cross-section areas A_{eff} and the effective section moduli W_{eff} is recommended in the determination of the cross-section resistances. Following the procedure provided in EN 1993-1-5 [52], the effective cross-section areas A_{eff} and the effective section moduli W_{eff} are calculated using eq. (14) and eq. (16). It should be noted that similar to the proposals made herein, [25, 32] also proposed the use of two section classes with the full and effective cross-section properties for the determination of the ultimate resistances of steel sections at elevated temperatures.

Different than the approaches provided in EN 1993-1-2 [28] and prEN 1993-1-2 [30], the proposed cross-section classification method and effective width formulae given by eq. (14) and eq. (16) employ the elevated temperature plate slendernesses $\bar{\lambda}_{p,\theta}$. This enables the consideration of the influence of the differential erosions of the strengths $k_{y,\theta}^*$ and stiffnesses $k_{E,\theta}$ at different elevated temperature levels on the response, thereby leading to more accurate estimations of the ultimate resistances of steel plates in fire as shown in the next section.

However, if this is deemed to result in an increased complexity by a designer, the dependency of cross-section classes and the effective width equations on elevated temperature levels can be conservatively eliminated by using the constant values of $\xi_\theta = \sqrt{k_{y,\theta}^*/k_{E,\theta}}$ provided in the expressions below in the determination of the elevated temperature plate slendernesses $\bar{\lambda}_{p,\theta}$ as given by eq. (18):

$$\begin{aligned}\xi_{\theta, const} &= \max\left(\sqrt{k_{y,\theta}^*/k_{E,\theta}}\right) \approx 1.0 \quad \text{for S690 steel,} \\ \xi_{\theta, const} &= \max\left(\sqrt{k_{y,\theta}^*/k_{E,\theta}}\right) \approx 1.2 \quad \text{for S460, S355, S275, S235 steel,}\end{aligned}\quad (22)$$

which were determined considering the maximum values of $\xi_\theta = \sqrt{k_{y,\theta}^*/k_{E,\theta}}$ within the elevated temperature range taken into account for the fire design of steel structures in practice.

5. Comparison of the new effective width method against EN 1993-1-2 and prEN 1993-1-2

In this section, the proposed effective width method is compared against the effective width methods provided in EN 1993-1-2 [28] and prEN 1993-1-2 [30] in terms of its accuracy and reliability for normal and high strength steel plates in fire. A wide range of parameters described Section 2.6 are taken into consideration, considering different plate slendernesses, loading conditions, elevated temperature levels and edge boundary conditions.

5.1. Assessment of the accuracy of the new effective width equations

Fig. 12, Fig. 13 and Fig. 14 show the accuracy of the proposed effective width method for the determination of the ultimate resistances of internal elements and outstand flanges under compression and internal elements in bending, considering grade S690 and S460 high strength steels and grade S355 and S235 normal strength steels as well as different plate slendernesses and elevated temperature levels. As can be seen from the figures, owing to the consideration of the differential erosions of the strengths and stiffnesses at different elevated temperature levels on the response by means of the elevated temperature plate slendernesses $\bar{\lambda}_{p,\theta}$, the proposed design rules lead to more accurate predictions of the ultimate strengths of high strength and normal strength steel plates in fire relative to EN 1993-1-2 [28] and prEN 1993-1-2 [30]. Moreover, as set out in Section 4, the proposed design equations utilise the modified elevated temperature yield strength reduction factor k_y^* , which enables the use of the elevated temperature ultimate strengths $f_{u,\theta} = k_{u,\theta} f_u$ in the cases where the elevated temperature strengths at 2% total strains $f_{y,\theta}$ are within the descending branches of the elevated temperature stress-strain curves; Fig. 12, Fig. 13 and Fig. 14 illustrate that this leads to an improved level of accuracy in the predictions of the ultimate resistances of grade S690 and S460 high strength steel plates relative to EN 1993-1-2 [28] and prEN 1993-1-2 [30]. The accuracy of the new effective width equations is compared against that of the effective width equations given in EN 1993-1-2 [28] and prEN 1993-1-2 [55] for high strength and

normal strength steel plates at elevated temperatures in Table 9 and Fig. 15 considering all the parameters described in Section 2.6. In Table 9 and Fig. 15, ζ is the ratio of the ultimate resistance obtained from the GMNIA of a steel plate R_{GMNIA} to that determined through a design method R_{method} (i.e. $\zeta = R_{GMNIA}/R_{method}$) and ζ_{av} , ζ_{COV} , ζ_{max} and ζ_{min} are the average, coefficient of variation (COV), maximum and minimum of ζ values, respectively. Note that the ultimate resistances determined by a design method R_{method} are denoted by R_{prop} , $R_{prEN1993-1-2}$ and $R_{EN1993-1-2}$ for the proposed design rules, prEN 1993-1-2 [30] and EN 1993-1-2 [28], respectively. As can be seen from Table 9 and Fig. 15, the proposed design rules provide more accurate ultimate strength predictions relative to EN 1993-1-2 [28] and prEN 1993-1-2 [30] for grade S690 and S460 high strength and grade S355, S275 and S235 normal steel plates at elevated temperatures.

The accuracy of the proposed design rules when they are applied using the constant $\xi_{\theta, const}$ factors given by eq. (22), which makes the proposed cross-section classification rules and effective width equations independent of elevated temperature levels, is also illustrated in Fig. 15 and Table 9 for all the considered parameters presented in Section 2.6, where R_{method} is denoted by $R_{prop, s}$. As can be seen from Fig. 15 and Table 9, when applied using the constant ξ_{θ} factors given by eq. (22), the proposed design rules also lead to ultimate strength predictions that are more accurate than those determined using the local buckling assessment rules provided in EN 1993-1-2 [28] and prEN1993-1-2 [55] for normal and high strength steel plates at elevated temperatures, thus illustrating the appropriateness of the use of the simplified version of the proposed design approach if it is preferred by a designer.

5.2. Reliability assessment

The reliability of the proposed design rules and that of EN 1993-1-2 [28] and prEN 1993-1-2 [30] is explored in Table 10, adopting the three reliability criteria proposed by Kruppa [56] for fire design methods of steel structures. According to Criterion 1 of [56], none of the ultimate strength estimations determined through a design method R_{method} should exceed those determined by the GMNIA of numerical models R_{GMNIA} by more than 15%, i.e. $(R_{method} - R_{GMNIA})/R_{GMNIA} \leq 15\%$. Criterion 2 of Kruppa [56] states that less than 20% of the design estimations should be on the unsafe side, i.e. $num(R_{method} > R_{GMNIA})/num(R_{method}) \leq 20\%$ and Criterion 3 of [56] indicates that the design predictions should be safe-sided on average, i.e. $\bar{X}[(R_{method} - R_{GMNIA})/R_{GMNIA}] \leq 0\%$. In Table 10, the percentage of the cases for which the overpredictions of resistances exceed 15% of those of GMNIA is shown under Criterion 1, the percentage of the cases for which resistances are overpredicted is shown under Criterion 2 and the average percentage of the differences between the design and GMNIA ultimate strengths is shown under Criterion 3. In the table, the violated reliability criteria are highlighted with ‘*’. Table 10 shows that the proposed design rules satisfy the Criterion 2 and Criterion 3 of Kruppa [56] for all the cases, though they very slightly violate the Criterion 1 of [56]. However, this was deemed to be acceptable as the reliability criterion is only violated by very small margins (0.35%-1.61%), which were only for internal elements under bending at the transitions between non-slender and slender classes (see Fig. 13), and the proposed effective width equations lead to both accurate and safe ultimate resistances of internal elements and outstand flanges as shown in Table 9 and

Fig. 15. The proposed effective width design equations will be applied to the design of high strength and normal strength steel sections in a future study where its accuracy and reliability for the design of high strength and normal strength steel cross-section in fire will be extensively assessed. Table 10 also shows the reliability of the proposed design rules when they are applied using the constant values of ξ_θ given by eq. (22), which makes the cross-section classification and effective width equations independent of elevated temperature levels. Similar observations made for the high reliability of the proposed design rules with varying ξ_θ can also be made for its simplified version applied with the constant $\xi_{\theta, const}$ values where the Criterion 2 was violated with a very small margin for grade S355 steel which is deemed acceptable with the satisfaction of the Criterion 1 for this case, thus illustrating the reliability of the simplified version of the proposed design rules. As can be seen in Table 10, EN 1993-1-2 [28] significantly violates the three reliability criteria of Kruppa [56] in almost all of the cases, while prEN 1993-1-2 [30] also violates the reliability criteria of [56] in a number of cases, thus highlighting that the developed effective width design approach results in more reliable local buckling strength predictions for high strength and normal strength steel plates at elevated temperatures relative to both EN 1993-1-2 [28] and prEN 1993-1-2 [30]

6. Conclusions

In this paper, the behaviour and design of grade S690 and S460 high strength and grade S355, S275 and S235 normal strength steel plates undergoing local buckling at elevated temperatures have been investigated. Shell finite element models of steel plates were created to replicate their response in fire, which were validated against experimental results from the literature. The validated shell finite element models of steel plates were then used to carry out comprehensive parametric studies, considering different elevated temperature levels, loading conditions, edge boundary conditions and plate slendernesses. The accuracy of the design rules provided in the existing European structural steel fire design standard EN 1993-1-2 [28] and its upcoming version prEN 1993-1-2 [30] was investigated using the extensive structural performance data obtained from the numerical parametric studies. It was observed that the existing local buckling assessment rules given in EN 1993-1-2 [28] lead to significant overestimations of the ultimate strengths of grade S690, S460 high strength and grade S355, S275 and S235 normal strength steel plates at elevated temperatures, while the updated local buckling assessment equations given in prEN 1993-1-2 [30] generally lead to safe ultimate strength predictions for grade S355, S275 and S235 normal strength plates but considerably underestimates the strengths of grade S690 and S460 high strength steel plates, thus leading to very uneconomic designs for the latter. With the aim of achieving accurate ultimate strength estimations for both high strength and normal strength steel plates in fire, new cross-section classification approach and effective width design equations were proposed. It was shown that owing to the consideration of the differential erosions of the strengths and stiffnesses at different elevated temperature levels unlike the design provisions given in EN 1993-1-2 [28] and prEN 1993-1-2 [30], the proposed design rules lead to accurate and safe ultimate strength predictions for both high strength steel and

normal strength steel plates in fire. The reliability of the proposed design rules and the local buckling assessment provisions provided in EN 1993-1-2 [28] and prEN 1993-1-2 [30] was also investigated adopting the three reliability criteria put forward by Kruppa [56] for fire design methods of steel structures. It was observed that the proposed design rules provide more reliable ultimate strength predictions relative to the design rules given in EN 1993-1-2 [28] and prEN 1993-1-2 [30] which both violated the reliability criteria of [56] in a high number of cases. In this paper, the structural response and design of individual high strength and normal strength steel plates in fire were investigated. Future research will be directed towards the investigation of the accuracy of the developed design rules for the ultimate resistance predictions of high strength and normal strength steel cross-sections at elevated temperatures.

References

- [1] EN 1993-1-12, Eurocode 3 Design of steel structures-Part 1-12: Additional rules for the extension of EN 1993 up to steel grades S 700. European Committee for Standardization (CEN), Brussels; 2007.
- [2] Standards Australia, AS 4100 steel structures. Australian Building Codes Board, Sydney; 1998.
- [3] Rasmussen, K.J., Hancock, G.J.. Plate slenderness limits for high strength steel sections. *Journal of Constructional Steel Research* 1992;23(1-3):73–96.
- [4] Shi, G., Zhou, W., Bai, Y., Lin, C.. Local buckling of 460 MPa high strength steel welded section stub columns under axial compression. *Journal of Constructional Steel Research* 2014;100:60–70.
- [5] Kim, D.K., Lee, C.H., Han, K.H., Kim, J.H., Lee, S.E., Sim, H.B.. Strength and residual stress evaluation of stub columns fabricated from 800 MPa high-strength steel. *Journal of Constructional Steel Research* 2014;102:111–120.
- [6] Shi, G., Xu, K., Ban, H., Lin, C.. Local buckling behavior of welded stub columns with normal and high strength steels. *Journal of Constructional Steel Research* 2016;119:144–153.
- [7] Wang, J., Afshan, S., Schillo, N., Theofanous, M., Feldmann, M., Gardner, L.. Material properties and compressive local buckling response of high strength steel square and rectangular hollow sections. *Engineering Structures* 2017;130:297–315.
- [8] Schillo, N., Taras, A., Feldmann, M.. Assessing the reliability of local buckling of plates for mild and high strength steels. *Journal of Constructional Steel Research* 2018;142:86–98.
- [9] Ma, J.L., Chan, T.M., Young, B.. Design of cold-formed high-strength steel tubular stub columns. *Journal of Structural Engineering* 2018;144(6):04018063.
- [10] Cao, X., Gu, L., Kong, Z., Zhao, G., Wang, M., Kim, S.E., et al. Local buckling of 800 MPa high strength steel welded T-section columns under axial compression. *Engineering Structures* 2019;194:196–206.
- [11] Chen, J., Young, B.. Design of high strength steel columns at elevated temperatures. *Journal of Constructional Steel Research* 2008;64(6):689–703.
- [12] Fang, H., Chan, T.M.. Axial compressive strength of welded S460 steel columns at elevated temperatures. *Thin-walled Structures* 2018;129:213–224.
- [13] Fang, H., Chan, T.M.. Resistance of axially loaded hot-finished S460 and S690 steel square hollow stub columns at elevated temperatures. *Structures* 2019;17:66–73.
- [14] Yang, K.C., Chen, S.J., Lin, C.C., Lee, H.H.. Experimental study on local buckling of fire-resisting steel columns under fire load. *Journal of Constructional Steel Research* 2005;61(4):553–565.
- [15] Yang, K.C., Lee, H.H., Chan, O.. Performance of steel H columns loaded under uniform temperature. *Journal of Constructional Steel Research* 2006;62(3):262–270.
- [16] Hirashima, T., Uesugi, H.. Load-bearing capacity of H-shaped steel columns under local buckling at elevated temperature. *Fire Safety Science* 2005;8:211–222.

- [17] Dharma, R.B., Tan, K.H.. Rotational capacity of steel I-beams under fire conditions Part I: Experimental study. *Engineering Structures* 2007;29(9):2391–2402.
- [18] Pauli, J., Somaini, D., Knobloch, M., Fontana, M.. Experiments on steel columns under fire conditions. IBK test report no. 340; Institute of Structural Engineering (IBK), ETH Zurich; 2012.
- [19] Pauli, J., Knobloch, M., Fontana, M.. On the local buckling behaviour of steel columns in fire. In: *Proceedings: 8th fib International PhD Symposium in Civil Engineering*, Kgs Lyngby, Denmark. Technical University of Denmark; 2010, p. 111–116.
- [20] Wang, W., Kodur, V., Yang, X., Li, G.. Experimental study on local buckling of axially compressed steel stub columns at elevated temperatures. *Thin-Walled Structures* 2014;82:33–45.
- [21] Prachar, M., Hricak, J., Jandera, M., Wald, F., Zhao, B.. Experiments of Class 4 open section beams at elevated temperature. *Thin-Walled Structures* 2016;98:2–18.
- [22] Quiel, S.E., Garlock, M.E.. Calculating the buckling strength of steel plates exposed to fire. *Thin-Walled Structures* 2010;48(9):684–695.
- [23] Seif, M., McAllister, T.. Stability of wide flange structural steel columns at elevated temperatures. *Journal of Constructional Steel Research* 2013;84:17–26.
- [24] Selamat, S., Garlock, M.E.. Plate buckling strength of steel wide-flange sections at elevated temperatures. *Journal of Structural Engineering* 2013;139(11):1853–1865.
- [25] Couto, C., Vila-Real, P., Lopes, N., Zhao, B.. Effective width method to account for the local buckling of steel thin plates at elevated temperatures. *Thin-Walled Structures* 2014;84:134–149.
- [26] Couto, C., Vila-Real, P., Lopes, N., Zhao, B.. Resistance of steel cross-sections with local buckling at elevated temperatures. *Journal of Constructional Steel Research* 2015;109:101–114.
- [27] Couto, C., Vila-Real, P., Lopes, N., Zhao, B.. Local buckling in laterally restrained steel beam-columns in case of fire. *Journal of Constructional Steel Research* 2016;122:543–556.
- [28] EN 1993-1-2, Eurocode 3 Design of steel structures-Part 1-2: General rules – Structural fire design. European Committee for Standardization (CEN), Brussels; 2005.
- [29] AISC 360-16, Specifications for structural steel buildings. American Institute of Steel Construction (AISC), Chicago; 2016.
- [30] Final Draft of EN 1993-1-2, Eurocode 3 Design of steel structures-Part 1-2: General rules – Structural fire design. European Committee for Standardization (CEN), Brussels; 2019.
- [31] Abaqus 2018 Reference Manual. Simulia, Dassault Systemes; 2018.
- [32] Xing, Z., Kucukler, M., Gardner, L.. Local buckling of stainless steel plates in fire. *Thin-Walled Structures* 2020;148:106570.
- [33] Bleich, F.. *Buckling strength of metal structures*. Mc Graw-Hill 1952;.
- [34] Timoshenko, S.P., Gere, J.M.. *Theory of Elastic Stability*. McGraw-Hill; 1961.
- [35] Trahair, N.S., Bradford, M., Nethercot, D., Gardner, L.. *The Behaviour and Design of Steel Structures to EC3*, fourth ed. CRC Press; 2008.
- [36] Kucukler, M.. Lateral instability of steel beams in fire: Behaviour, numerical modelling and design. *Journal of Constructional Steel Research* 2020;170:106095.
- [37] Kucukler, M.. Compressive resistance of high-strength and normal-strength steel CHS members at elevated temperatures. *Thin-Walled Structures* 2020;152:106753.
- [38] Kucukler, M., Xing, Z., Gardner, L.. Behaviour and design of stainless steel I-section columns in fire. *Journal of Constructional Steel Research* 2020;165:105890.
- [39] Kucukler, M., Gardner, L.. Design of web-tapered steel beams against lateral-torsional buckling through a stiffness reduction method. *Engineering Structures* 2019;190:246–261.
- [40] Kucukler, M., Gardner, L., Macorini, L.. Lateral-torsional buckling assessment of steel beams through a stiffness reduction method. *Journal of Constructional Steel Research* 2015;109:87–100.
- [41] Agarwal, A., Choe, L., Varma, A.H.. Fire design of steel columns: Effects of thermal gradients. *Journal of Constructional Steel Research* 2014;93:107–118.
- [42] Crisfield, M.A.. A fast incremental/iterative solution procedure that handles “snap-through”. *Computers & Structures* 1981;13(1-3):55–62.
- [43] Ramm, E.. Strategies for tracing the nonlinear response near limit points. In: *Nonlinear finite element*

- analysis in structural mechanics. Springer; 1981, p. 63–89.
- [44] Rubert, A., Schaumann, P.. Structural steel and plane frame assemblies under fire action. *Fire Safety Journal* 1986;10(3):173–184.
 - [45] Schneider, R., Lange, J.. Constitutive equations of structural steel S460 at high temperatures. In: *Nordic Steel Construction Conference Proceedings*, Malmo, Sweden. 2009, p. 204–211.
 - [46] Choi, I.R., Chung, K.S., Kim, D.H.. Thermal and mechanical properties of high-strength structural steel HSA800 at elevated temperatures. *Materials & Design* 2014;63:544–551.
 - [47] Xiong, M.X., Liew, J.R.. Mechanical properties of heat-treated high tensile structural steel at elevated temperatures. *Thin-Walled Structures* 2016;98:169–176.
 - [48] Mirambell, E., Real, E.. On the calculation of deflections in structural stainless steel beams: An experimental and numerical investigation. *Journal of Constructional Steel Research* 2000;54(1):109–133.
 - [49] Qiang, X., Bijlaard, F., Kolstein, H.. Dependence of mechanical properties of high strength steel S690 on elevated temperatures. *Construction and Building Materials* 2012;30:73–79.
 - [50] Qiang, X., Bijlaard, F.S., Kolstein, H.. Elevated-temperature mechanical properties of high strength structural steel S460N: Experimental study and recommendations for fire-resistance design. *Fire Safety Journal* 2013;55:15–21.
 - [51] Qiang, X.. Behaviour of high strength steel endplate connections in fire and after fire. Ph.D. thesis; Delft University of Technology; 2013.
 - [52] EN 1993-1-5, Eurocode 3 Design of steel structures-Part 1-5: Plated structural elements. European Committee for Standardization (CEN), Brussels; 2005.
 - [53] Bradford, M.A., Liu, X.. Flexural-torsional buckling of high-strength steel beams. *Journal of Constructional Steel Research* 2016;124:122–131.
 - [54] EN 1993-1-1, Eurocode 3 Design of steel structures-Part 1-1: General rules and rules for buildings. European Committee for Standardization (CEN), Brussels; 2005.
 - [55] prEN 1993-1-1, Final Draft of Eurocode 3 Design of steel structures-Part 1-1: General rules and rules for buildings. European Committee for Standardization (CEN), Brussels; 2018.
 - [56] Kruppa, J.. Eurocodes–Fire parts: Proposal for a methodology to check the accuracy of assessment methods. CEN TC 250, Horizontal Group Fire, Document no: 99/130; 1999.

Figures captions

Figure 1 : Stress-strain relationship and material property reduction factors for normal strength steel at elevated temperatures adopted in this study as given in [28]

Figure 2 : Comparison of the Young's modulus reduction factors $k_{E,\theta}$ and yield strength reduction factors $k_{y,\theta}$ for grade S690, S460, S355, S275 and S235 steels adopted in this study

Figure 3 : Elevated temperature stress-strain response of S690 and S460 grade steels at different elevated temperature levels obtained by [49, 50] and material model adopted in the finite element models

Figure 4 : Boundary conditions adopted in the finite element models of internal elements and outstand flanges

Figure 5 : Lowest buckling modes used in the application of geometric imperfections to the finite element models of internal elements and outstand flanges

Figure 6 : Influence of residual stresses on the ultimate resistances of normal strength and high strength steel internal elements and outstand flanges at elevated temperatures

Figure 7 : Variation of $\sqrt{k_{E,\theta}/k_{y,\theta}}$ at different elevated temperature levels for high strength and normal strength steels

Figure 8 : Effective width method used to determine the ultimate resistances of steel plates

Figure 9 : Accuracy of EN 1993-1-2 [28] and prEN1993-1-2 [30] for the predictions of the ultimate strengths of normal strength and high strength steel internal elements under compression at elevated temperatures

Figure 10 : Accuracy of EN 1993-1-2 [28] and prEN 1993-1-2 [30] for the predictions of the ultimate strengths of normal strength and high strength steel internal elements under bending at elevated temperatures

Figure 11 : Accuracy of EN 1993-1-2 [28] and prEN 1993-1-2 [30] for the predictions of the ultimate strengths of normal strength and high strength steel outstand flanges under compression at elevated temperatures

Figure 12 : Accuracy of the proposed effective width equations for the predictions of the ultimate strengths of normal strength and high strength steel internal elements under compression at elevated temperatures

Figure 13 : Accuracy of the proposed effective width equations for the predictions of the ultimate strengths of normal strength and high strength steel internal elements under bending at elevated temperatures

Figure 14 : Accuracy of the proposed effective width equations for the predictions of the ultimate strengths of normal strength and high strength steel outstand flanges under compression at elevated temperatures

Figure 15 : Accuracy of EN 1993-1-2 [28], prEN 1993-1-2 [30] and the full and simplified versions of the proposed effective width equations for ultimate strength predictions of grade S690 and S460 high strength and grade S355, S275 and S235 steel internal elements and outstand flanges at elevated temperatures

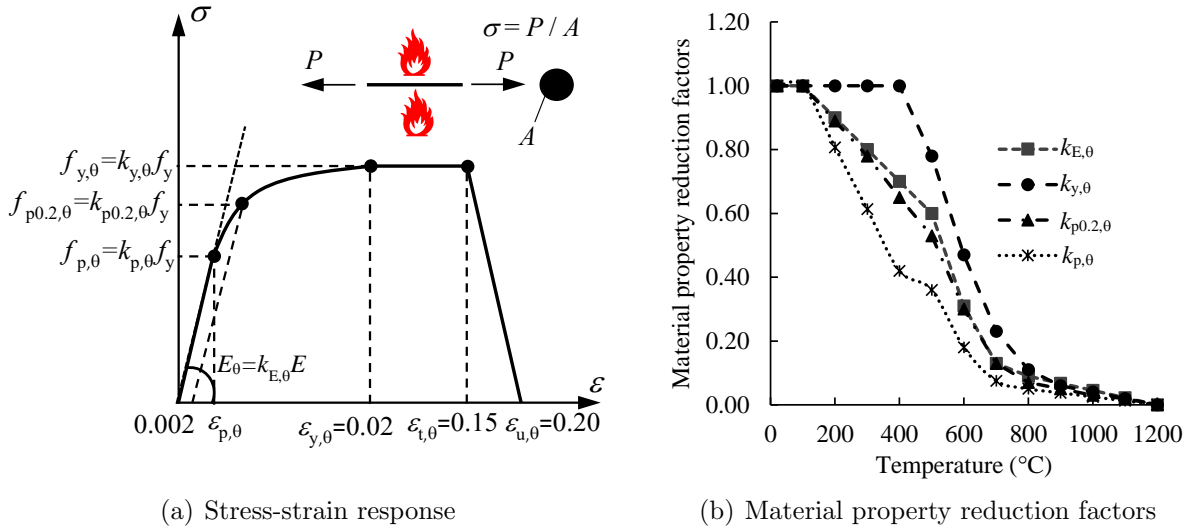


Figure 1: Stress-strain relationship and material property reduction factors for normal strength steel at elevated temperatures adopted in this study as given in [28]

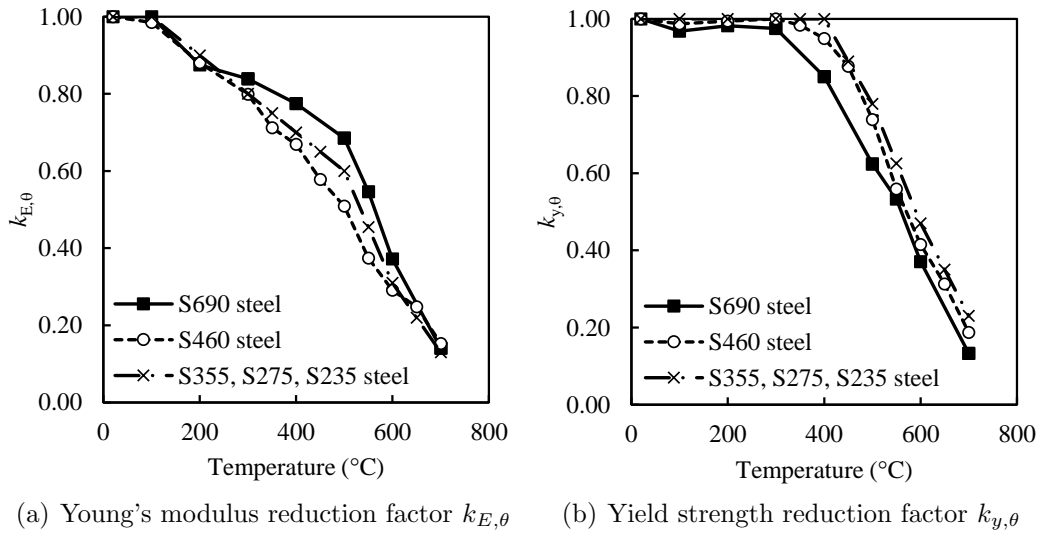
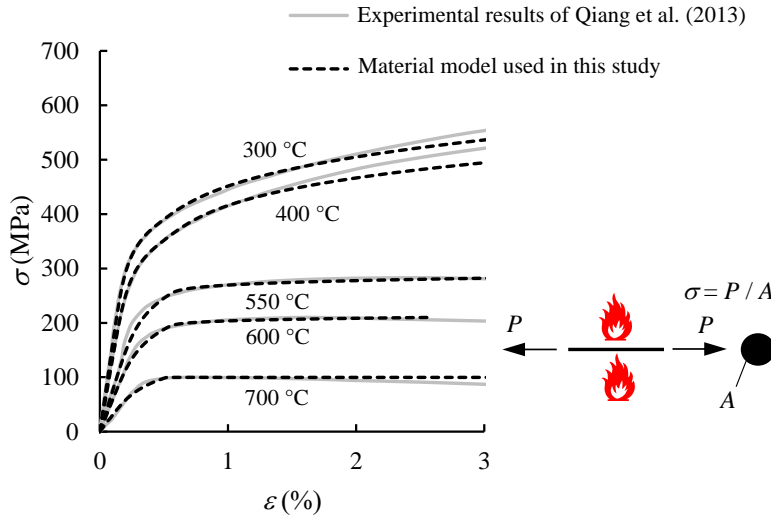
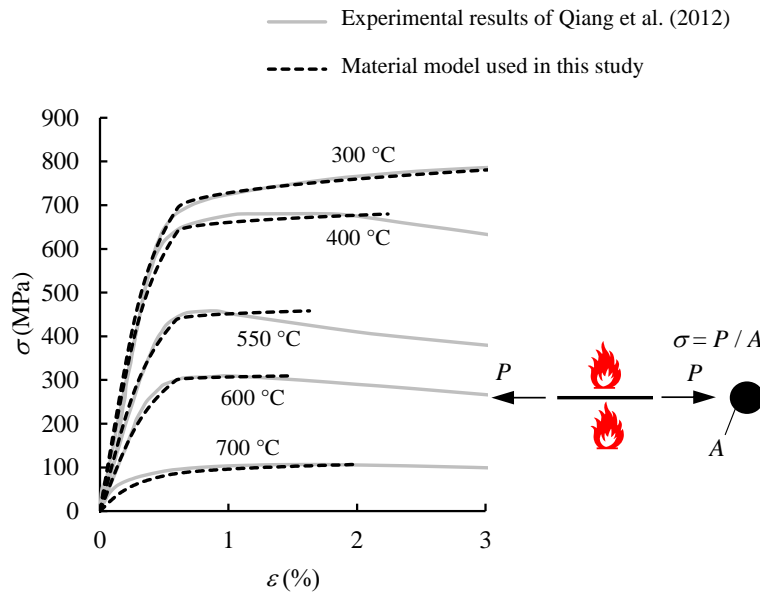


Figure 2: Comparison of the Young's modulus reduction factors $k_{E,\theta}$ and yield strength reduction factors $k_{y,\theta}$ for grade S690, S460, S355, S275 and S235 steels adopted in this study

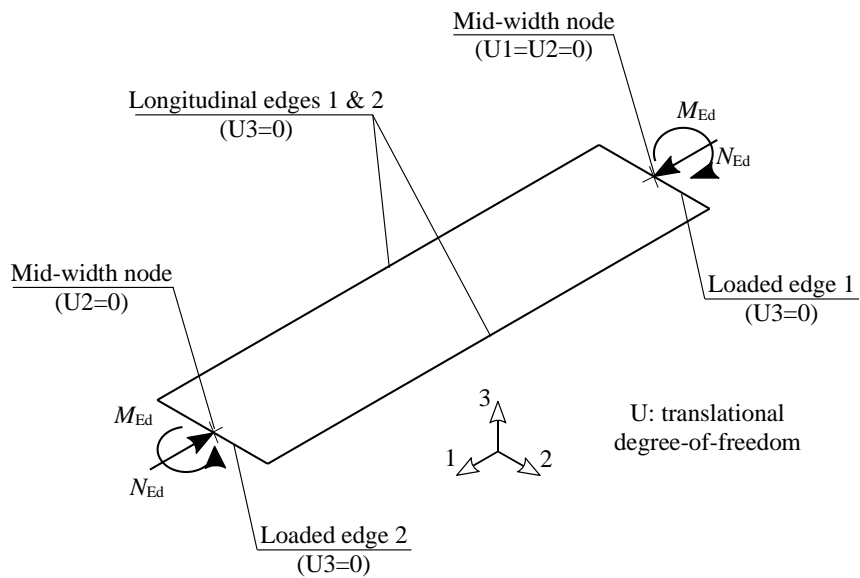


(a) S460

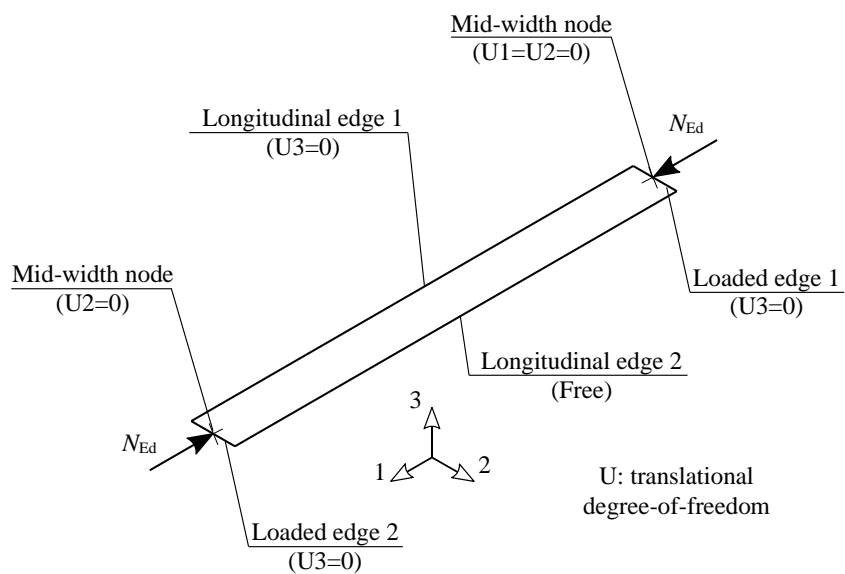


(b) S690

Figure 3: Elevated temperature stress-strain response of S690 and S460 grade steels at different elevated temperature levels obtained by [49, 50] and material model adopted in the finite element models

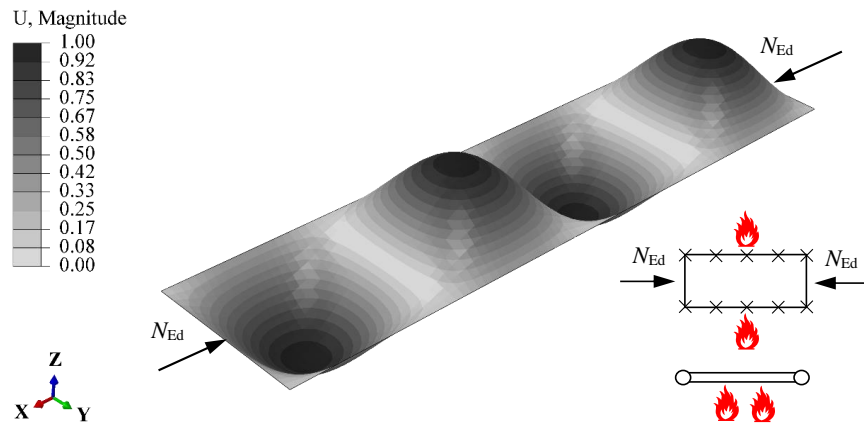


(a) Internal element

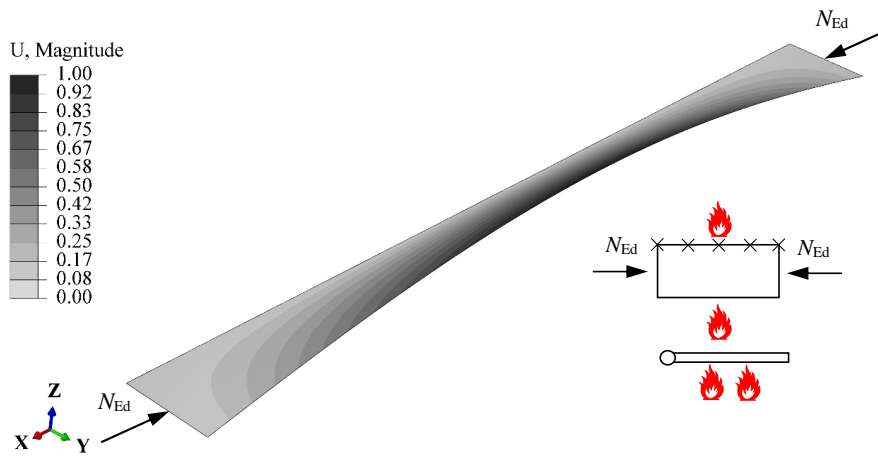


(b) Outstand flange

Figure 4: Boundary conditions adopted in the finite element models of internal elements and outstand flanges



(a) Internal element



(b) Outstand flange

Figure 5: Lowest buckling modes used in the application of geometric imperfections to the finite element models of internal elements and outstand flanges

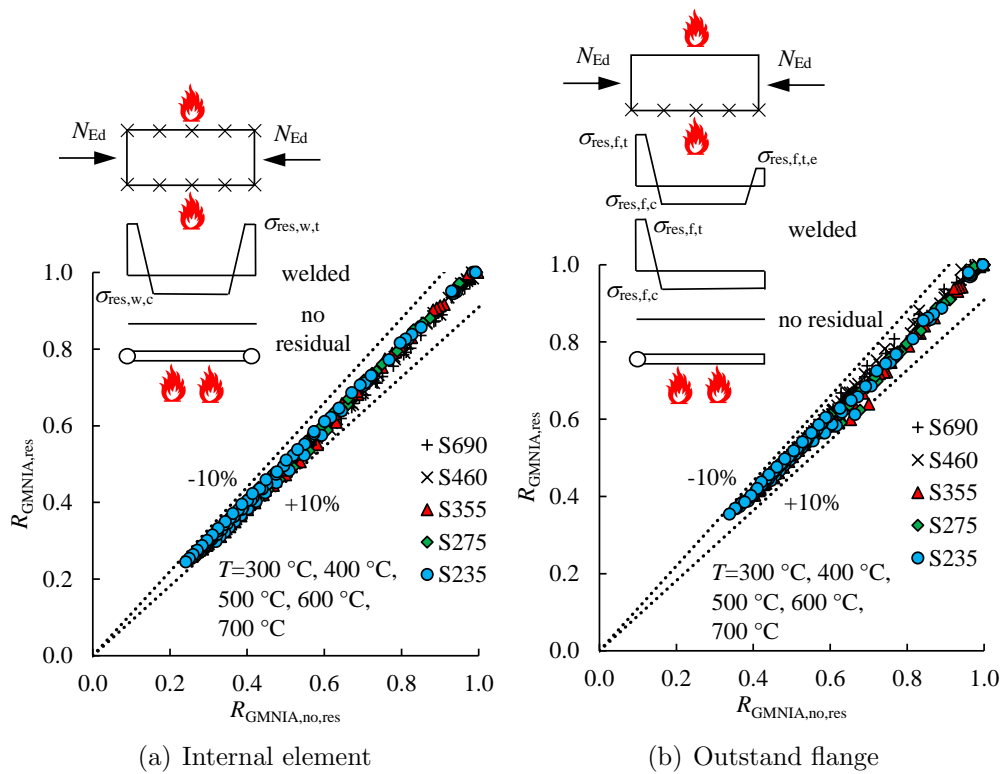


Figure 6: Influence of residual stresses on the ultimate resistances of normal strength and high strength steel internal elements and outstand flanges at elevated temperatures

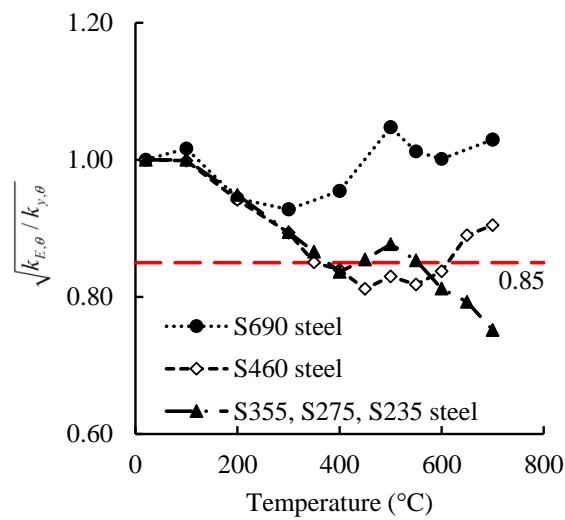


Figure 7: Variation of $\sqrt{k_{E,\theta}/k_{y,\theta}}$ at different elevated temperature levels for high strength and normal strength steels

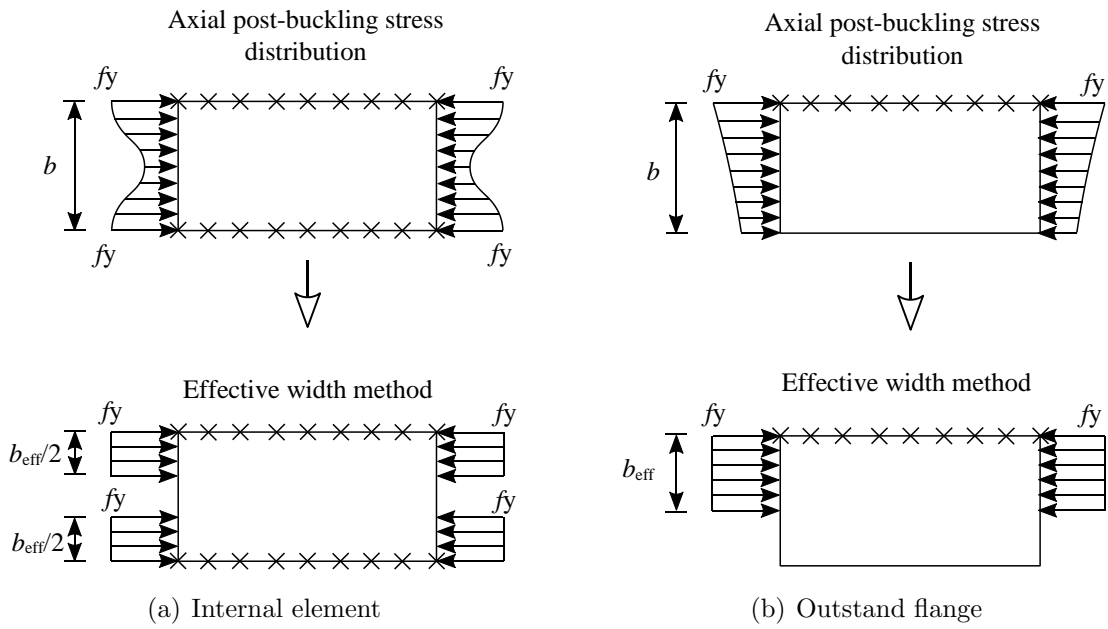


Figure 8: Effective width method used to determine the ultimate resistances of steel plates

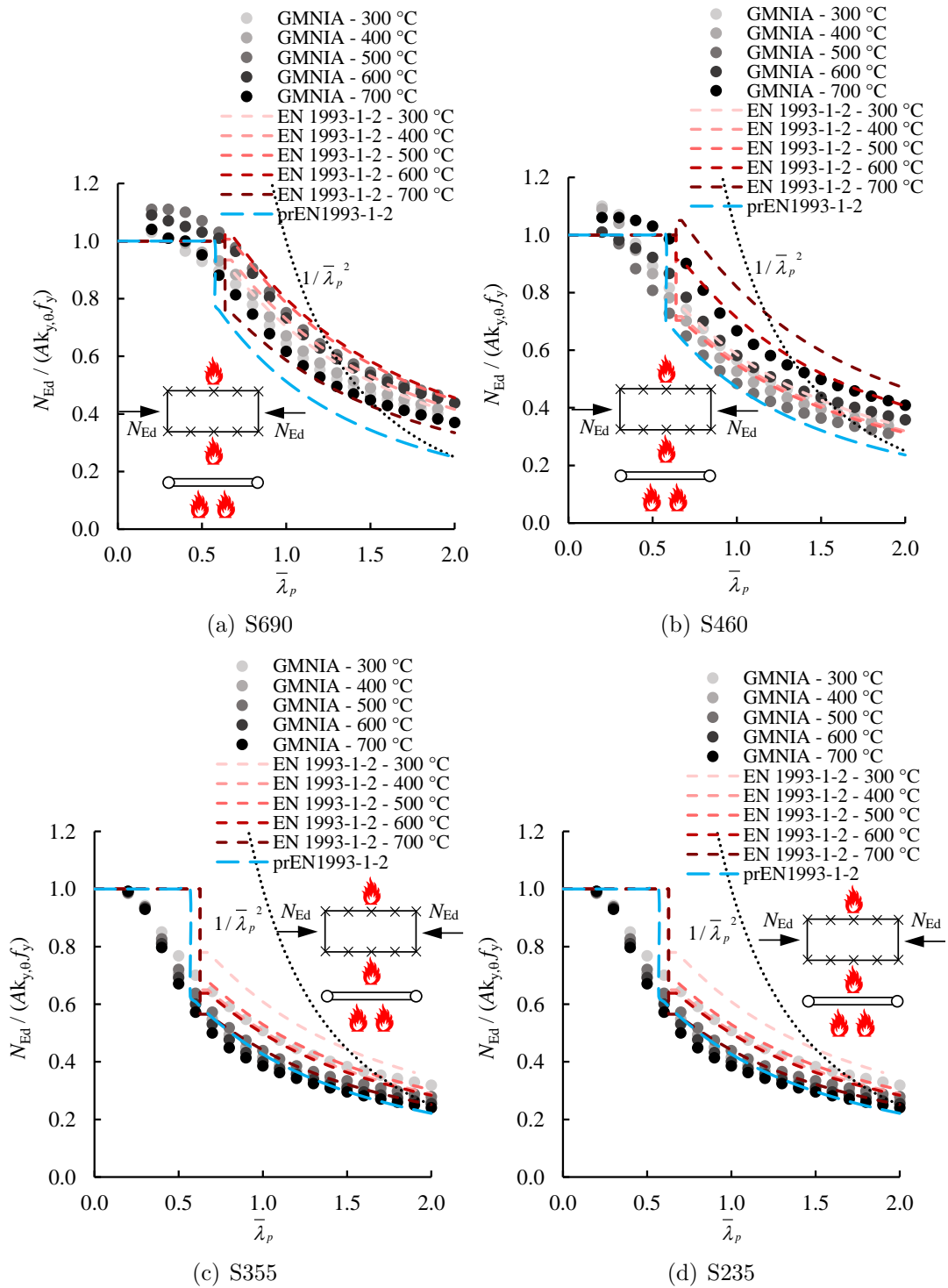


Figure 9: Accuracy of EN 1993-1-2 [28] and prEN1993-1-2 [30] for the predictions of the ultimate strengths of normal strength and high strength steel internal elements under compression at elevated temperatures

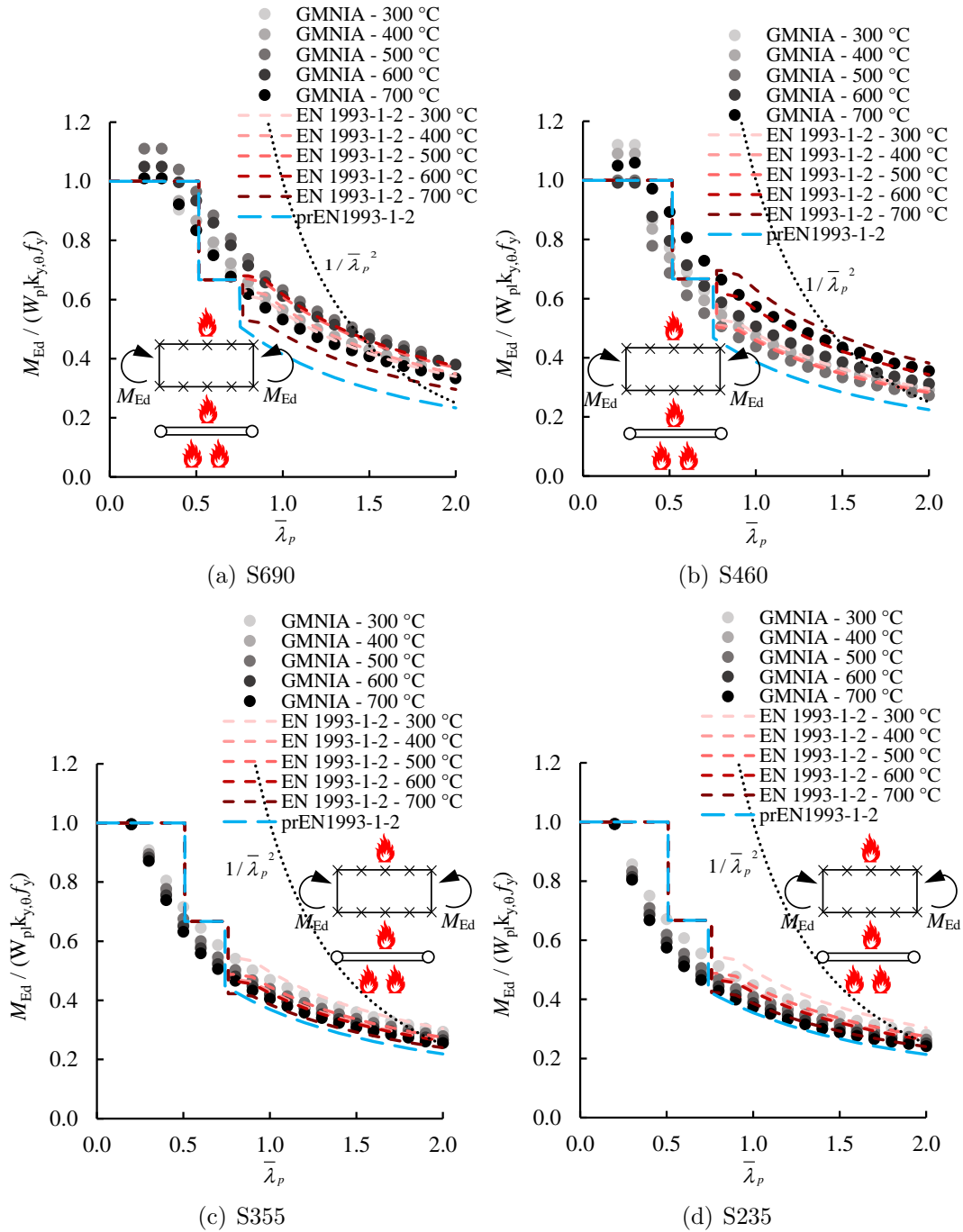


Figure 10: Accuracy of EN 1993-1-2 [28] and prEN 1993-1-2 [30] for the predictions of the ultimate strengths of normal strength and high strength steel internal elements under bending at elevated temperatures

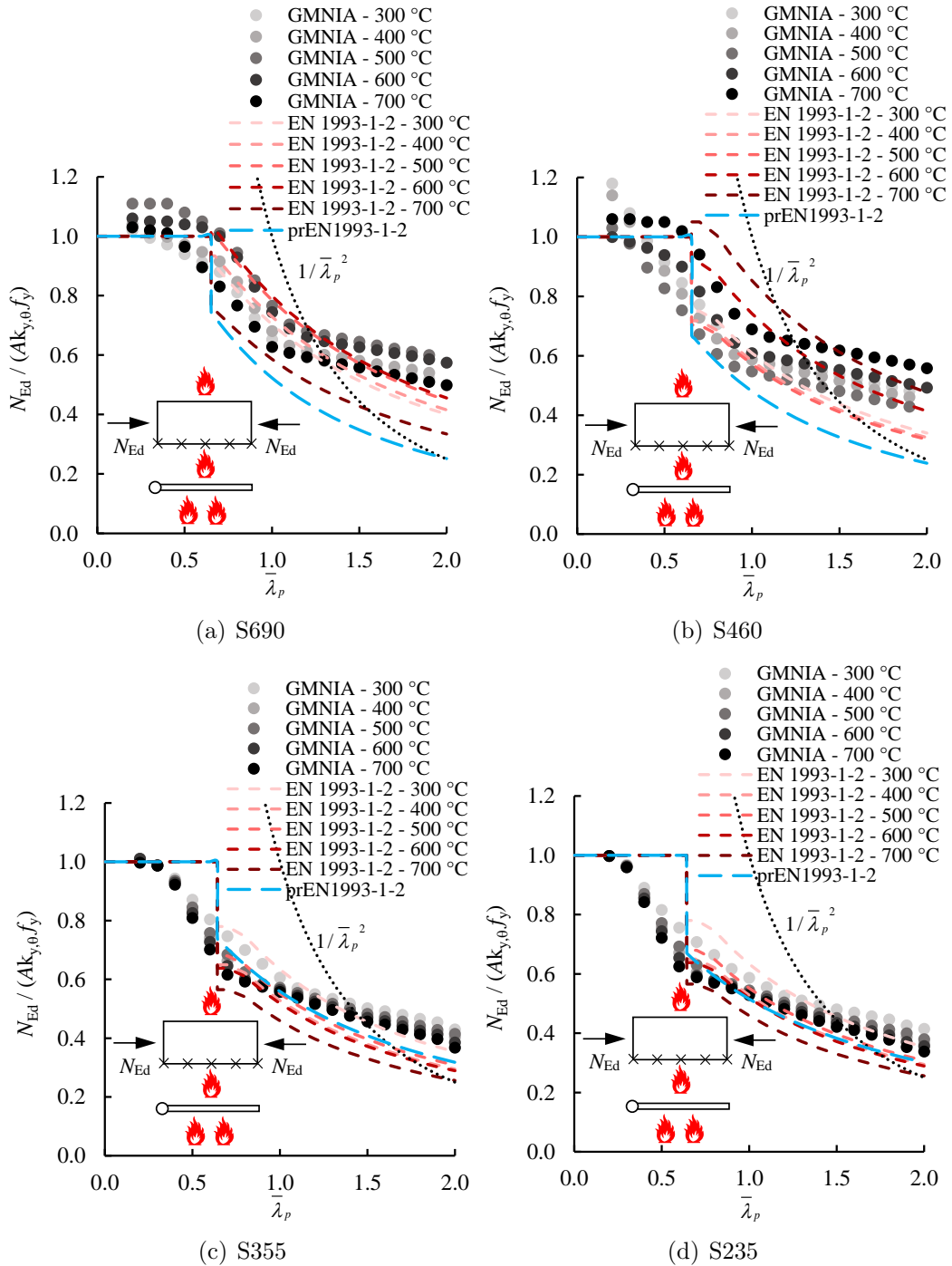


Figure 11: Accuracy of EN 1993-1-2 [28] and prEN 1993-1-2 [30] for the predictions of the ultimate strengths of normal strength and high strength steel outstand flanges under compression at elevated temperatures

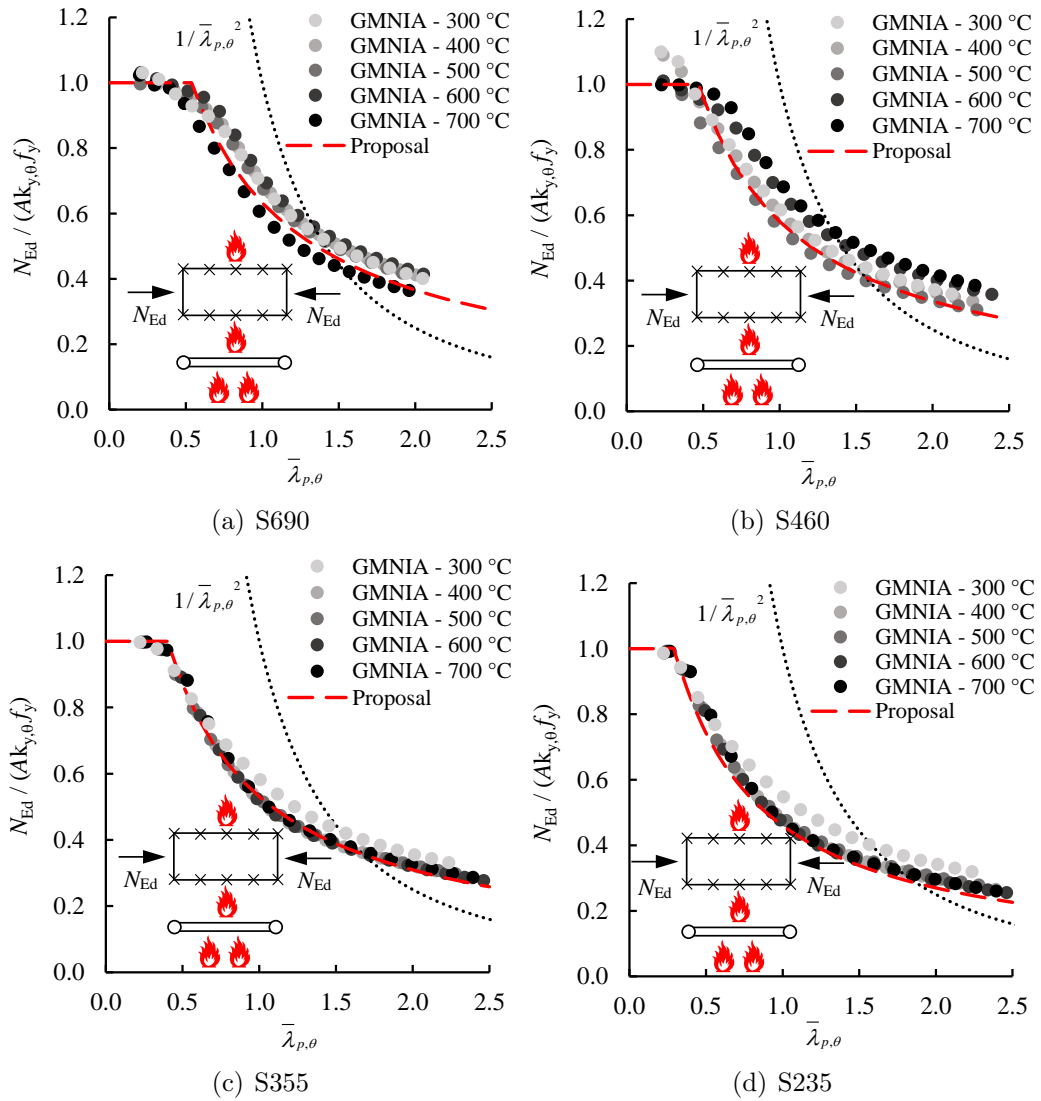


Figure 12: Accuracy of the proposed effective width equations for the predictions of the ultimate strengths of normal strength and high strength steel internal elements under compression at elevated temperatures

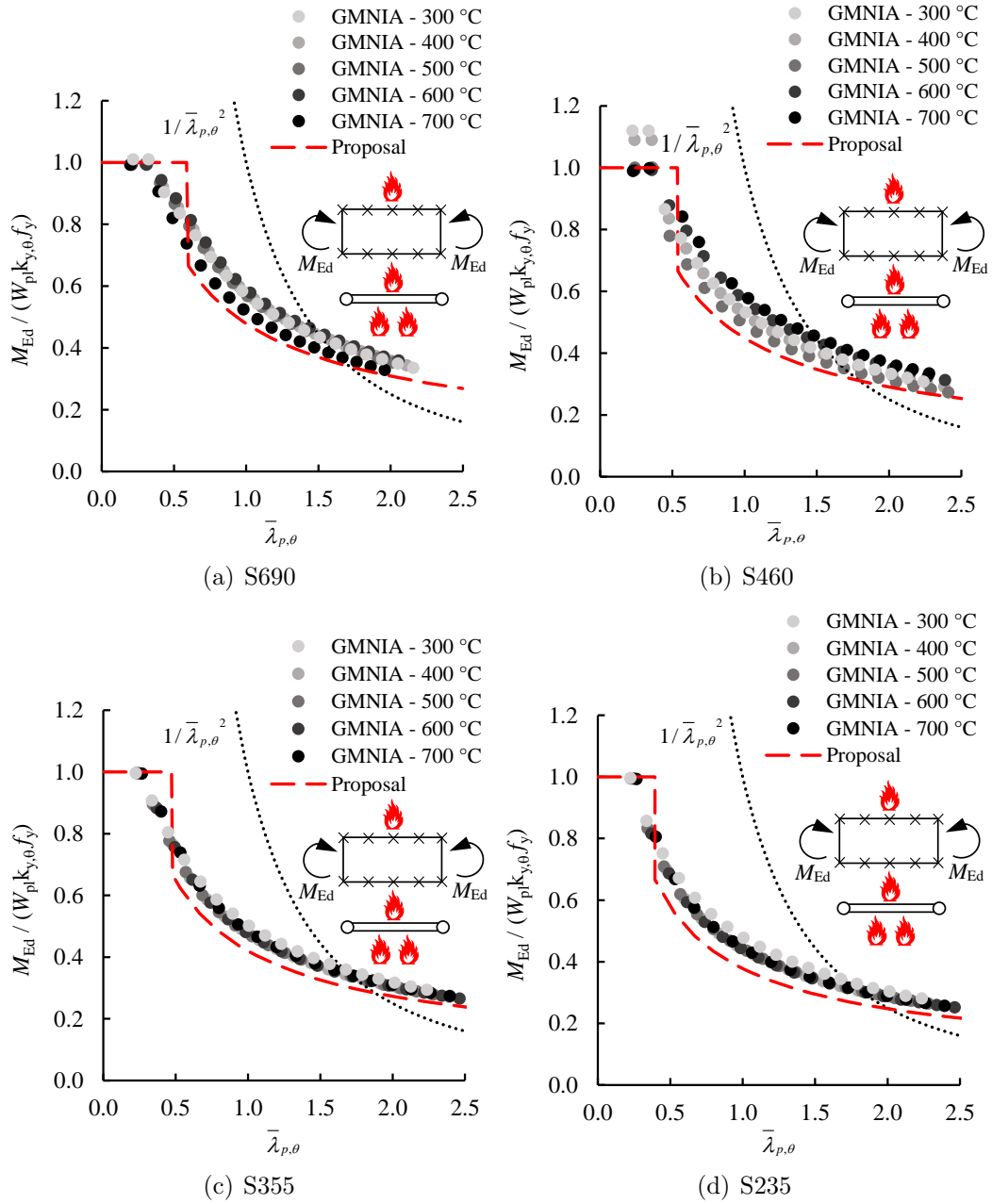


Figure 13: Accuracy of the proposed effective width equations for the predictions of the ultimate strengths of normal strength and high strength steel internal elements under bending at elevated temperatures

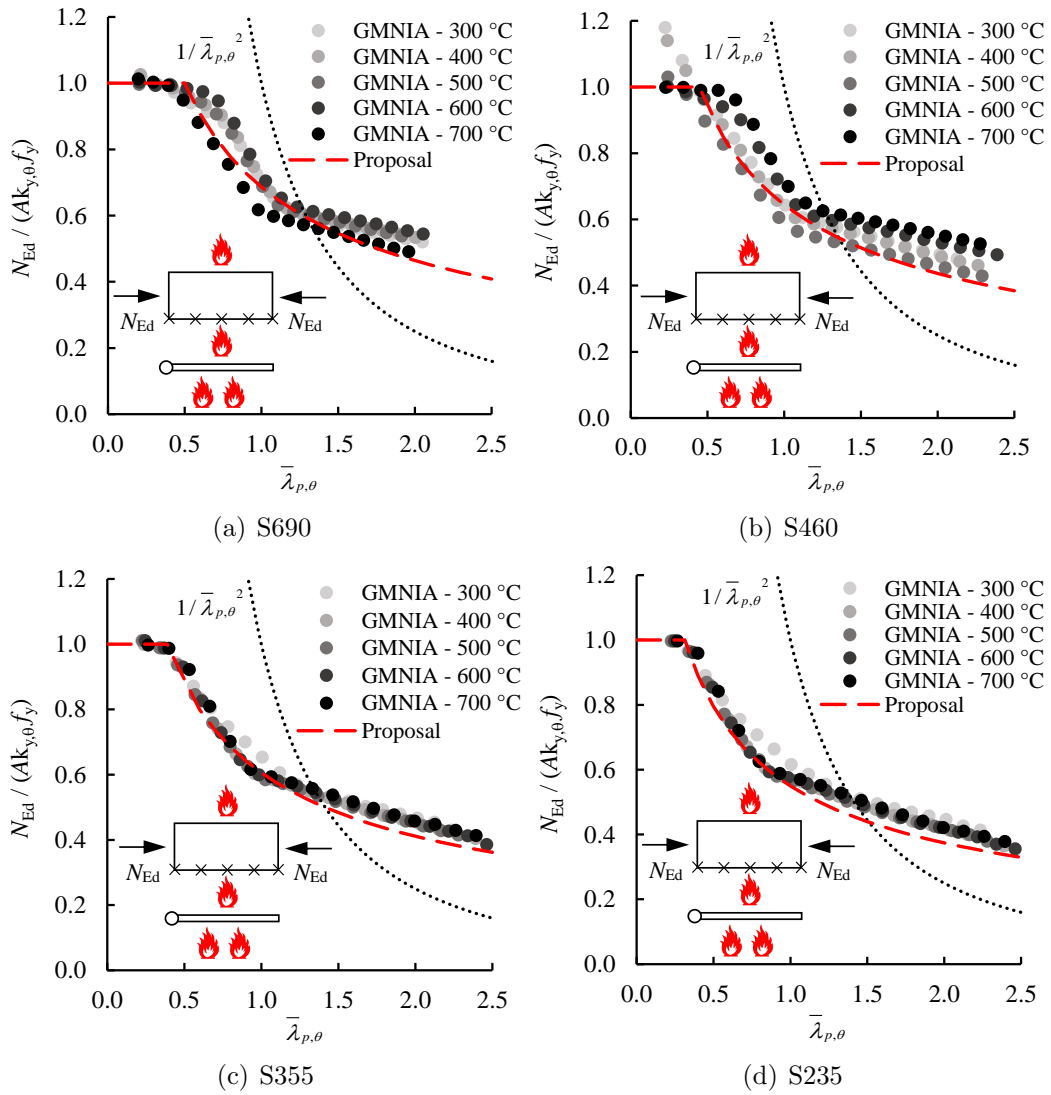


Figure 14: Accuracy of the proposed effective width equations for the predictions of the ultimate strengths of normal strength and high strength steel outstand flanges under compression at elevated temperatures

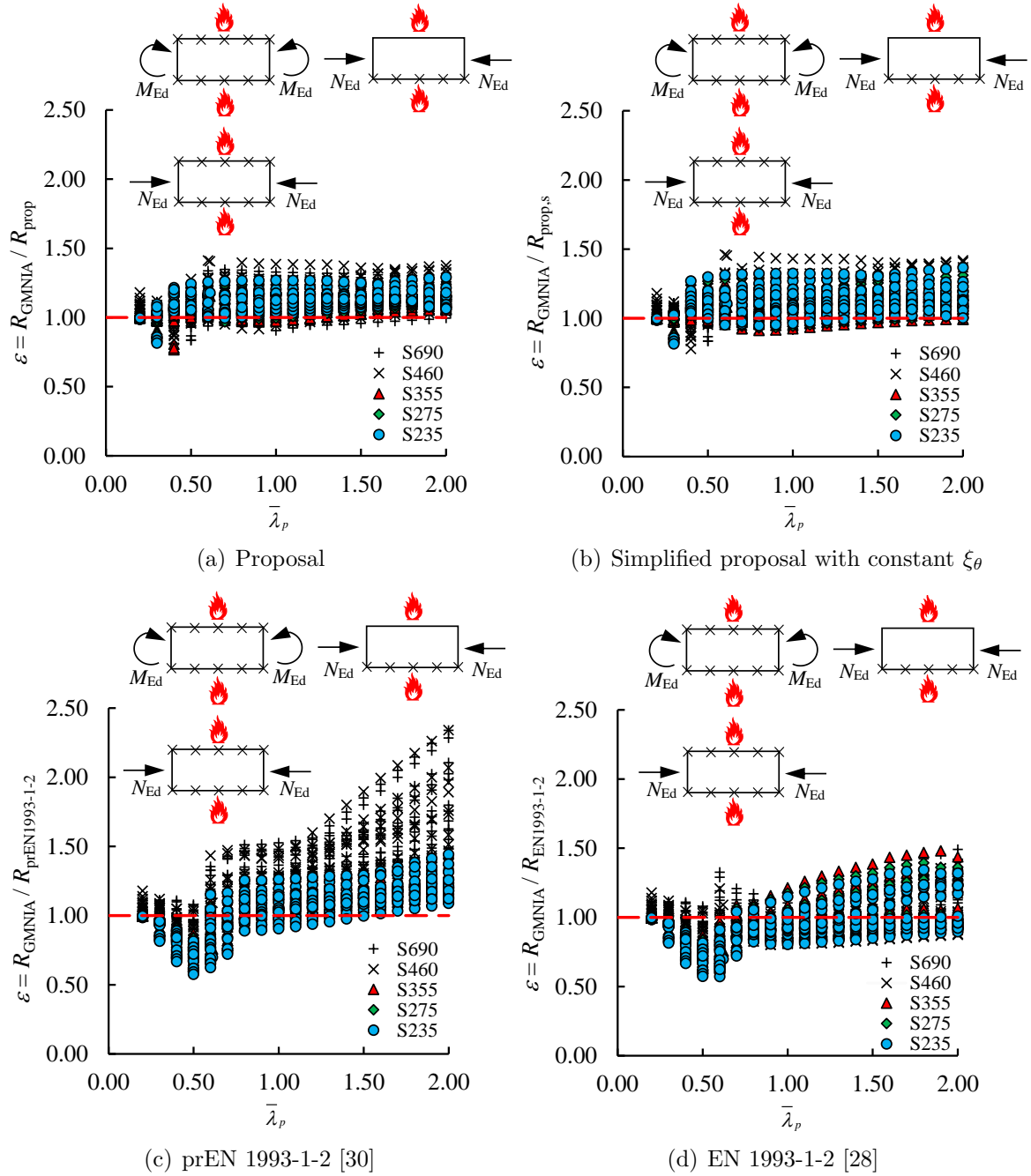


Figure 15: Accuracy of EN 1993-1-2 [28], prEN 1993-1-2 [30] and the full and simplified versions of the proposed effective width equations for ultimate strength predictions of grade S690 and S460 high strength and grade S355, S275 and S235 steel internal elements and outstand flanges at elevated temperatures

Tables captions

Table 1 : Material reduction factors derived by Qiang et al. [49] and Ramberg-Osgood exponents used in this study for grade S690 steel ($E = 204690$ MPa, $f_y=789$ MPa, $\sigma_u=821$ MPa and $\epsilon_u=0.051$)

Table 2 : Material reduction factors derived by Qiang et al. [50] and Ramberg-Osgood exponents used in this study for grade S460 steel ($E = 202812$ MPa, $f_y=504$ MPa, $\sigma_u=640$ MPa and $\epsilon_u=0.115$)

Table 3 : Comparison of the ultimate resistances obtained through the experiments of Wang et al. [20] and those determined through the finite element models developed in this study

Table 4 : Comparison of the ultimate resistances obtained through the experiments of Pauli et al. [18] and those determined through the finite element models developed in this study

Table 5 : Summary of the parametric studies carried out in this paper

Table 6 : The limit width-to-thickness ratios for the classification of cross-section elements at room temperature according to EN 1993-1-1 [54] and prEN 1993-1-1 [55]

Table 7 : Cross-section resistances of Class 1, 2, 3 and 4 sections in fire according to EN 1993-1-1 [54] and prEN 1993-1-1 [55]

Table 8 : Cross-section resistances of non-slender and slender sections according to the proposed design method

Table 9 : Assessment of the accuracy of the proposed design rules, their simplified version and the design rules provided in EN 1993-1-2 [28] and prEN 1993-1-2 [30] for the ultimate strength predictions of high strength and normal strength steel internal elements and out-stand flanges at elevated temperatures

Table 10 : Assessment of the reliability of the proposed design rules, their simplified version and the design rules provided in EN 1993-1-2 [28] and prEN 1993-1-2 [30] for the ultimate strength predictions of high strength and normal strength steel plates in fire on the basis of the reliability criteria set out by Kruppa [56]. Note that a number denoted by * violates the corresponding criterion

Table 1: Material reduction factors derived by Qiang et al. [49] and Ramberg-Osgood exponents used in this study for grade S690 steel ($E = 204690$ MPa, $f_y=789$ MPa, $\sigma_u=821$ MPa and $\epsilon_u=0.051$)

Temperature ($^{\circ}\text{C}$)	$k_{E,\theta}$	$k_{p0.2,\theta}$	$k_{y,\theta}$	$k_{u,\theta}$	$k_{\epsilon_u,\theta}$	n_θ	m_θ
200	0.875	0.884	0.982	0.991	0.957	6.20	1.93
300	0.839	0.879	0.975	0.961	0.696	5.80	2.10
400	0.775	0.794	0.850	0.828	0.280	5.40	2.27
500	0.685	0.628	0.624	0.628	0.161	5.00	2.43
550	0.546	0.554	0.533	0.558	0.178	4.80	2.52
600	0.372	0.380	0.371	0.377	0.196	4.60	2.60
700	0.141	0.100	0.133	0.130	0.333	4.20	2.77

Table 2: Material reduction factors derived by Qiang et al. [50] and Ramberg-Osgood exponents used in this study for grade S460 steel ($E = 202812$ MPa, $f_y=504$ MPa, $\sigma_u=640$ MPa and $\epsilon_u=0.115$)

Temperature ($^{\circ}\text{C}$)	$k_{E,\theta}$	$k_{p0.2,\theta}$	$k_{y,\theta}$	$k_{u,\theta}$	$k_{\epsilon_u,\theta}$	n_θ	m_θ
200	0.881	0.812	0.994	0.969	0.758	10.00	2.70
300	0.799	0.750	1.000	1.000	0.804	9.00	3.00
400	0.669	0.681	0.949	0.880	0.517	8.00	3.30
500	0.509	0.520	0.739	0.601	0.296	7.00	3.60
550	0.374	0.496	0.559	0.443	0.217	6.50	3.75
600	0.291	0.379	0.415	0.328	0.139	6.00	3.90
700	0.153	0.196	0.187	0.157	0.066	5.00	4.20

Table 3: Comparison of the ultimate resistances obtained through the experiments of Wang et al. [20] and those determined through the finite element models developed in this study

Cross-section	Steel grade	Critical plate	Temperature ($^{\circ}\text{C}$)	$N_{u,test}$ (kN)	$N_{u,FE}$ (kN)	$N_{u,FE}/N_{u,test}$
I-316 \times 200 \times 6 \times 8	S235	Internal element	20	1247	1170	0.94
			450	830	685	0.83
			650	280	234	0.84
I-336 \times 160 \times 8 \times 8	S460	Internal element	20	2269	2022	0.89
			450	1450	1260	0.87
			650	430	521	1.21
I-250 \times 250 \times 6 \times 8	S235	Outstand flange	20	1375	1580	1.15
			450	930	867	0.93
			650	295	289	0.98
I-250 \times 220 \times 8 \times 8	S460	Outstand flange	20	2637	2375	0.90
			450	1650	1498	0.91
			650	430	578	1.34

Table 4: Comparison of the ultimate resistances obtained through the experiments of Pauli et al. [18] and those determined through the finite element models developed in this study

Cross-section	Steel grade	Critical plate	Temperature (°C)	$N_{u,test}$ (kN)	$N_{u,FE}$ (kN)	$N_{u,FE}/N_{u,test}$
			20	1214	1169	0.96
SHS 160 × 160 × 5	S355	Internal element	400	795	801	1.01
			550	468	505	1.08
			700	138	172	1.25

Table 5: Summary of the parametric studies carried out in this paper

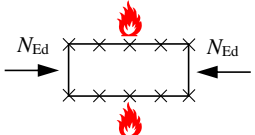
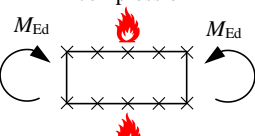
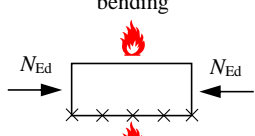
Loading and boundary conditions	Steel grades	Temperature	Plate slenderness $\bar{\lambda}_p$
 <p>Internal element under compression</p>			0.2, 0.3, 0.4, 0.5
 <p>Internal element under bending</p>	S690 S460 S355 S275 S235	300 °C 400 °C 500 °C 600 °C 700 °C	0.6, 0.7, 0.8, 0.9, 1.0, 1.1, 1.2, 1.3, 1.4, 1.5, 1.6, 1.7, 1.8, 1.9, 2.0
 <p>Outstand flange under compression</p>			

Table 6: The limit width-to-thickness ratios for the classification of cross-section elements at room temperature according to EN 1993-1-1 [54] and prEN 1993-1-1 [55]

Cross-section element	EN 1993-1-1			prEN 1993-1-1		
	Class 1	Class 2	Class 3	Class 1	Class 2	Class 3
Internal element under compression	33 ϵ	38 ϵ	42 ϵ	28 ϵ	34 ϵ	38 ϵ
Internal element under bending	72 ϵ	83 ϵ	124 ϵ	72 ϵ	83 ϵ	121 ϵ
Outstand element under compression	9 ϵ	10 ϵ	14 ϵ	9 ϵ	10 ϵ	14 ϵ

Table 7: Cross-section resistances of Class 1, 2, 3 and 4 sections in fire according to EN 1993-1-1 [54] and prEN 1993-1-1 [55]

Cross-section class	Design resistance under compression $N_{fi,t,Rd}$		Design resistance under bending $M_{fi,t,Rd}$	
	EN 1993-1-2	prEN 1993-1-2	EN 1993-1-2	prEN 1993-1-2
Class 1 & 2	$Ak_{y,\theta}f_y/\gamma_{M,fi}$	$Ak_{y,\theta}f_y/\gamma_{M,fi}$	$W_{pl}k_{y,\theta}f_y/\gamma_{M,fi}$	$W_{pl}k_{y,\theta}f_y/\gamma_{M,fi}$
Class 3	$Ak_{y,\theta}f_y/\gamma_{M,fi}$	$Ak_{y,\theta}f_y/\gamma_{M,fi}$	$W_{el}k_{y,\theta}f_y/\gamma_{M,fi}$	$W_{el}k_{y,\theta}f_y/\gamma_{M,fi}$
Class 4	$A_{eff}k_{p0.2,\theta}f_y/\gamma_{M,fi}$	$A_{eff}k_{y,\theta}f_y/\gamma_{M,fi}$	$W_{eff}k_{p0.2,\theta}f_y/\gamma_{M,fi}$	$W_{eff}k_{y,\theta}f_y/\gamma_{M,fi}$

Table 8: Cross-section resistances of non-slender and slender sections according to the proposed design method

Cross-section class	Design resistance under compression	Design resistance under bending
Non-slender	$N_{fi,t,Rd} = Ak_{y,\theta}^*f_y/\gamma_{M,fi}$	$M_{fi,t,Rd} = W_{pl}k_{y,\theta}^*f_y/\gamma_{M,fi}$
Slender	$N_{fi,t,Rd} = A_{eff}k_{y,\theta}^*f_y/\gamma_{M,fi}$	$M_{fi,t,Rd} = W_{eff}k_{y,\theta}^*f_y/\gamma_{M,fi}$

Table 9: Assessment of the accuracy of the proposed design rules, their simplified version and the design rules provided in EN 1993-1-2 [28] and prEN 1993-1-2 [30] for the ultimate strength predictions of high strength and normal strength steel internal elements and outstand flanges at elevated temperatures

Design method	Steel grade	N	ζ_{av}	ζ_{COV}	ζ_{max}	ζ_{min}
Proposal	S690	285	1.11	0.097	1.35	0.83
	S460	285	1.12	0.106	1.41	0.78
	S355	285	1.07	0.067	1.20	0.77
	S275	285	1.09	0.066	1.24	0.85
	S235	285	1.11	0.069	1.29	0.82
Simplified proposal with constant ξ_θ	S690	285	1.10	0.095	1.34	0.83
	S460	285	1.14	0.116	1.46	0.78
	S355	285	1.07	0.076	1.26	0.88
	S275	285	1.09	0.083	1.31	0.85
	S235	285	1.11	0.088	1.37	0.82
prEN 1993-1-2 [30]	S690	285	1.38	0.210	2.34	0.83
	S460	285	1.28	0.223	2.34	0.69
	S355	285	1.08	0.149	1.45	0.63
	S275	285	1.06	0.158	1.45	0.60
	S235	285	1.05	0.165	1.44	0.58
EN 1993-1-2 [28]	S690	285	1.03	0.102	1.49	0.83
	S460	285	0.98	0.126	1.39	0.69
	S355	285	1.00	0.157	1.48	0.63
	S275	285	0.96	0.158	1.39	0.60
	S235	285	0.93	0.159	1.34	0.57

Table 10: Assessment of the reliability of the proposed design rules, their simplified version and the design rules provided in EN 1993-1-2 [28] and prEN 1993-1-2 [30] for the ultimate strength predictions of high strength and normal strength steel plates in fire on the basis of the reliability criteria set out by Kruppa [56]. Note that a number denoted by * violates the corresponding criterion

Design method	Steel grade	Criterion 1	Criterion 2	Criterion 3
Proposal	S690	0.71*	16.61	-9.53
	S460	0.71*	14.13	-10.16
	S355	1.06*	19.83	-5.81
	S275	0.35*	10.56	-7.97
	S235	1.06*	7.75	-9.54
Simplified proposal with constant ξ_θ	S690	0.71*	17.67	-8.19
	S460	0.71*	13.07	-11.41
	S355	0.00	20.24*	-6.11
	S275	0.35*	13.51	-7.81
	S235	1.06*	11.97	-9.39
prEN 1993-1-2 [30]	S690	0.70*	8.10	-24.34
	S460	4.24*	14.49	-18.37
	S355	10.21*	32.75*	-4.78
	S275	12.68*	34.51*	-2.85
	S235	14.79*	37.32*	-1.36
EN 1993-1-2 [28]	S690	0.70*	42.61*	-2.43
	S460	14.13*	60.42*	3.54*
	S355	11.97*	60.21*	2.76*
	S275	16.55*	75.70*	7.30*
	S235	26.06*	80.28*	10.12*